

NATIONAL ADVISORY COMMITTEE FOR AERONAUTICS

TECHNICAL NOTE 2654

TWO-DIMENSIONAL FLOW ON GENERAL SURFACES OF

REVOLUTION IN TURBOMACHINES

By John D. Stanitz and Gaylord O. Ellis

Lewis Flight Propulsion Laboratory
Cleveland, Ohio



Washington

March 1952

AFB :
TECHNICAL LIBRARY
AFL 2311



NATIONAL ADVISORY COMMITTEE FOR AERONAUTICS

TECHNICAL NOTE 2654

TWO-DIMENSIONAL FLOW ON GENERAL SURFACES OF

REVOLUTION IN TURBOMACHINES

By John D. Stanitz and Gaylord O. Ellis

SUMMARY

A method of analysis is developed for two-dimensional flow on general surfaces of revolution in turbomachines with arbitrary blade shapes. The method of analysis is developed for steady, compressible, nonviscous, irrotational flow that is assumed uniform normal to the surfaces of revolution. Incompressible solutions on a mean surface of revolution between the hub and shroud are presented for four flow rates through each of two centrifugal impellers with the same hub-shroud contours but with different blade spacings. In addition, correlation equations are developed whereby the velocity components and the stream function distribution can be predicted for compressible or incompressible flow in straight-bladed impellers only, with any tip speed, flow rate, area variation, blade spacing, and for any flow surface of revolution.

INTRODUCTION

In order to achieve substantial improvements in compressor and turbine efficiency, new methods of design must be developed, and these methods should be based on detailed knowledge of flow conditions within turbomachines (compressors and turbines). The purpose of the analysis method developed at the NACA Lewis laboratory and presented in this report is to provide a tool whereby increased knowledge of the flow characteristics in turbomachines can be acquired. In addition the two-dimensional numerical results presented in this report provide the basis for future comparison with the results of three-dimensional solutions.

Several two-dimensional methods of analysis have already been developed (references 1 and 2, for example). In general, these various methods differ in technique and scope of application. In particular, in reference 2 a method of analysis is developed for two-dimensional compressible flow in turbomachines with conic flow surfaces generated about the axis of the turbomachine by straight lines. In this report

the analysis method of reference 2 is extended to include arbitrary surfaces of revolution generated about axes of turbomachines. In addition correlation equations are developed for the rapid estimation of flow conditions in impellers with straight blades.

METHOD OF ANALYSIS

Preliminary Considerations

For given compressor operating conditions, a complete solution for the flow through turbomachines depends on the machine geometry (three-dimensional effects) and on the fluid properties (compressibility and viscosity). The effects of compressibility are considered in the analysis method of this report but the effects of viscosity are not. Some three-dimensional effects are indicated by the combination of two-dimensional solutions. The idea of these quasi-three-dimensional solutions is considered next.

Quasi-three-dimensional solutions. - Consider the flow of an ideal fluid through a typical passage between blades such as shown in figure 1. The fluid is free to follow whatever path the pressure and inertia forces require of it. If, however, the number of blades in the turbomachine is considered to approach infinity, the space between blades, as well as the blade thickness, approaches zero and the path of the fluid is limited to the curved mean surface of the blade. The fluid motion is thus reduced from a general three-dimensional motion to a two-dimensional motion restricted to the mean blade surface. The streamlines of this two-dimensional motion can be projected on the meridional plane (axial-radial plane) as shown in figure 2. The solutions are axially symmetrical because the infinite number of blades prevent the fluid properties from varying about the axis of the turbomachine.

Axial-symmetry solutions establish mean circumferential flow conditions, but for finite blade spacing flow conditions vary circumferentially, as well as from hub to shroud. In order to investigate the circumferential variation, which is superimposed on the circumferential mean flow conditions obtained by the axial-symmetry solution, it is assumed that the flow is limited to surfaces of revolution generated by rotating the meridional streamlines of the axial-symmetry solution (fig. 2) about the axis of the turbomachine. If these meridional streamlines are selected with sufficiently close spacing, flow conditions can be considered uniform normal to these surfaces of revolution. Thus the flow is limited to two-dimensional motion on flow surfaces of revolution.

Blade-to-blade solutions can be obtained for every flow surface of revolution generated by the streamlines in the meridional plane. Therefore, flow conditions can be determined approximately throughout the

2466 passage. This resulting quasi-three-dimensional solution is obtained by the combination of two types of two-dimensional solution: axial-symmetry solution and blade-to-blade solution. Although this combination of two-dimensional solutions does not result in a rigorous three-dimensional solution, because, for example, the flow has been constrained to surfaces of revolution, the combination must result in a better picture of the true flow conditions than does either of the two-dimensional solutions alone. Analysis methods for the axial-symmetry type of solution are developed in references 3 and 4, for example. In this report analysis methods are developed for the blade-to-blade type of solution on flow surfaces of revolution generated around the axis of the turbomachine by known, or assumed, streamlines in the meridional plane.

Coordinates. - The cylindrical coordinates R , θ , and Z shown in figure 3 are convenient to use in theoretical studies of the flow in turbomachines. (All symbols are defined in the appendix.) These coordinates are dimensionless, the linear coordinates R and Z having been divided by the blade-tip radius r_T (so that R equals 1.0 at the blade tip, for example). The coordinate system rotates with the blade row about the Z -axis. The angular velocity ω is always considered positive and in the counterclockwise direction as shown in figure 3.

Velocity components. - The velocity Q relative to the rotating coordinate system has components Q_R , Q_θ , and Q_Z in the R , θ , and Z directions, respectively (fig. 3). These velocities are dimensionless, having been divided by the stagnation speed of sound c_0 upstream of the blade row, where

$$c_0^2 = \gamma g R^* T_0 \quad (1)$$

In equation (1) R^* is the gas constant, γ is the ratio of specific heats, and T_0 is the stagnation (total) temperature upstream of the blade row. The blade-tip speed is likewise dimensionless and becomes the conventional blade-tip Mach number M_T , which is defined by

$$M_T = \frac{\omega r_T}{c_0} \quad (2)$$

Thus the tangential velocity of the blade at any radius R is equal to RM_T and the absolute tangential velocity of the fluid is equal to $(RM_T + Q_\theta)$.

In addition to the three components of the relative velocity Q_R , Q_θ , and Q_Z it is convenient to define a fourth velocity component, lying in the meridional plane (RZ-plane) and defined as the meridional velocity Q_M , where from figure 3

$$Q_M^2 = Q_R^2 + Q_Z^2 \quad (3)$$

The meridional velocity Q_M helps define the angle α , shown in figure 3, from which figure

$$Q_R = Q_M \sin \alpha \quad (4)$$

$$Q_Z = Q_M \cos \alpha \quad (5)$$

Thermodynamic relations. - From the general energy equation, in the absence of heat transfer, it can be shown that along a streamline the static (stream) temperature T is related to the relative velocity Q by (reference 2)

$$\frac{T}{T_0} = 1 + \frac{\gamma-1}{2} \left[(RM_T)^2 - Q^2 - 2M_T\lambda_U \right] \quad (6)$$

where the subscript U refers to conditions far upstream of the blade row and where λ is the whirl ratio defined as the absolute moment of momentum divided by $r_T c_0$ and given by

$$\lambda = R(RM_T + Q_\theta) \quad (7)$$

For isentropic flow the pressure ratio P and the density ratio ρ/ρ_0 are likewise related to the relative velocity Q by

$$P = \frac{p}{p_0} = \left(\frac{T}{T_0} \right)^{\frac{\gamma}{\gamma-1}} = \left\{ 1 + \frac{\gamma-1}{2} \left[(RM_T)^2 - Q^2 - 2M_T\lambda_U \right] \right\}^{\frac{\gamma}{\gamma-1}} \quad (8)$$

and

$$\frac{\rho}{\rho_0} = \left(\frac{T}{T_0} \right)^{\frac{1}{\gamma-1}} = \left\{ 1 + \frac{\gamma-1}{2} \left[(RM_T)^2 - Q^2 - 2M_T\lambda_U \right] \right\}^{\frac{1}{\gamma-1}} \quad (9)$$

where p and ρ are the static pressure and density, respectively.

Analysis

A streamline that was obtained from an axial-symmetry solution in the meridional plane (fig. 2, for example) is shown in figure 4 together with the coordinates, velocities, and so forth at a point on the streamline. At this point a tangent to the streamline in the meridional plane intersects the axis of the turbomachine with the angle α , as indicated. If this tangent line is rotated about the axis, it generates the surface of a cone that is tangent to the flow surface of revolution obtained by rotating the streamline (fig. 4). At the circumferential line of tangency a fluid particle on the flow surface of revolution is also on the conic flow surface. This fluid particle is shown in figure 5 on a developed view of the cone surface. The height ratio H of the fluid particle is defined by

$$H = \frac{h}{h_T} \quad (10)$$

where h (fig. 2) is the local spacing between center lines of the channels formed by the adjacent streamlines (fig. 2) on either side of the streamline that generates the surface of revolution.

Absolute irrotational motion. - In the absence of shock, viscous effects, and so forth, the absolute motion of the fluid everywhere on the surface of revolution is isentropic and hence irrotational so that the absolute circulation $d\Gamma$ around every fluid particle is zero and from figure 5

$$d\Gamma = 0 = \frac{\partial}{\partial R} \left[(RM_T + Q_\theta) R d\theta \right] dR - \frac{\partial}{\partial \theta} \left[\frac{Q_M dR}{\sin \alpha} \right] d\theta$$

from which

$$0 = 2RM_T \sin \alpha + Q_\theta \sin \alpha + R \sin \alpha \frac{\partial Q_\theta}{\partial R} - \frac{\partial Q_M}{\partial \theta} \quad (11)$$

Continuity. - From continuity considerations for the fluid particle in figure 5

$$\frac{\partial}{\partial R} \left(\frac{\rho}{\rho_0} Q_M H R \right) + \frac{\partial}{\partial \theta} \left(\frac{\rho}{\rho_0} Q_\theta \frac{H}{\sin \alpha} \right) = 0 \quad (12)$$

where H is a function of R along the surface of revolution

$$H = H(R)$$

A stream function ψ satisfies the continuity equation (12) if defined as

$$\left. \begin{aligned} \frac{\partial \psi}{\partial \theta} &= \frac{\rho}{\rho_0} Q_M H R \\ \frac{\partial \psi}{\partial R} &= - \frac{\rho}{\rho_0} Q_\theta \frac{H}{\sin \alpha} \end{aligned} \right\} \quad (13)$$

Transformation of coordinates. - For convenience in the relaxation solution the following transformation of coordinates is introduced:

$$d\xi = \frac{1}{(\Delta\theta) \sin \alpha} \frac{dR}{R} \quad (14a)$$

and

$$d\eta = \frac{d\theta}{\Delta\theta} \quad (14b)$$

where $\Delta\theta$ is the angular spacing of the blades about the axis of the turbomachine. Equation (14a) can be integrated to give ξ as a function of R with ξ arbitrarily equal to zero when R equals one, and equation (14b) can be integrated to give η equal to $\frac{\theta}{\Delta\theta}$. By this transformation, which is conformal, the curved flow surface of revolution becomes a flat plane ($\xi\eta$ -plane). Lines of constant ξ and η are shown transformed onto a flow surface of revolution in figure 6. The problem is solved in the $\xi\eta$ -plane and transformed back to the curved flow surface of revolution. The advantages of this transformation are: first, a warping of the blade shape which for straight blades results in straight parallel boundaries (blades) in the transformed plane, thus permitting equal grid spacing for solution by relaxation methods; and second, a reduction in the number of terms in the final differential equation for the stream function distribution, thus reducing the labor involved in obtaining a relaxation solution.

General differential equation for stream function distribution. - In terms of the transformed coordinates, equation (11) for absolute irrotational motion becomes

$$0 = 2RM_T \Delta\theta \sin \alpha + Q_\theta \Delta\theta \sin \alpha + \frac{\partial Q_\theta}{\partial \xi} - \frac{\partial Q_M}{\partial \eta} \quad (15)$$

and equation (13) for the stream function becomes

$$\left. \begin{aligned} \frac{\partial \psi}{\partial \eta} &= \frac{\rho}{\rho_0} Q_M HR (\Delta\theta) \\ \frac{\partial \psi}{\partial \xi} &= - \frac{\rho}{\rho_0} Q_\theta HR (\Delta\theta) \end{aligned} \right\} \quad (16)$$

Equations (15) and (16) combine to give (note that H and R are independent of η)

$$\begin{aligned} \frac{\partial^2 \psi}{\partial \xi^2} + \frac{\partial^2 \psi}{\partial \eta^2} - \frac{\partial \ln H}{\partial \xi} \frac{\partial \psi}{\partial \xi} - \frac{\partial \ln \frac{\rho}{\rho_0}}{\partial \xi} \frac{\partial \psi}{\partial \xi} - \frac{\partial \ln \frac{\rho}{\rho_0}}{\partial \eta} \frac{\partial \psi}{\partial \eta} - \\ 2 \frac{\rho}{\rho_0} HR^2 (\Delta\theta)^2 M_T \sin \alpha = 0 \end{aligned} \quad (17)$$

In this equation the density ratio $\frac{\rho}{\rho_0}$ is related to the velocity components Q_M and Q_θ by equation (9) where $Q^2 = Q_M^2 + Q_\theta^2$, and the velocity components are related to the stream function ψ by equation (16). This system of equations ((9), (16), and (17)) can be solved for given boundary conditions by relaxation methods (references 2 and 5) to give the distribution of ψ for two-dimensional flow past arbitrary blade shapes on the flow surface of revolution. The velocity components, and therefore the pressure, density, and so forth, can be obtained from the distribution of ψ by means of equation (16).

Incompressible flow. - For incompressible flow the stagnation speed of sound contained in the definition of Q and M_T is undefined and its use can be eliminated by considering the ratio $\frac{Q}{M_T}$, which is the ratio of the relative velocity to the impeller tip speed. Thus, with $\frac{\rho}{\rho_0}$ equal to one for incompressible flow equation (16) becomes

$$\left. \begin{aligned} \frac{\partial \psi_i}{\partial \eta} &= \frac{Q_M}{M_T} HR (\Delta\theta) \\ \frac{\partial \psi_i}{\partial \xi} &= - \frac{Q_\theta}{M_T} HR (\Delta\theta) \end{aligned} \right\} \quad (16a)$$

where from equations (16) ψ_1 is related to ψ by

$$\psi_1 = \frac{\psi}{M_T}$$

so that equation (17) becomes after dividing by M_T

$$\frac{\partial^2 \psi_1}{\partial \xi^2} + \frac{\partial^2 \psi_1}{\partial \eta^2} - \frac{\partial \ln H}{\partial \xi} \frac{\partial \psi_1}{\partial \xi} - 2HR^2 (\Delta\theta)^2 \sin \alpha = 0 \quad (17a)$$

which is the partial differential equation used for the numerical solutions presented in this report.

Method of Solution

Numerical methods. - Solutions of the differential equations (17) or (17a) for given blade shapes on given, arbitrary surfaces of revolution and for given flow rates and blade-tip Mach numbers are obtained by relaxation methods using techniques discussed in reference 2.

Boundary considerations. - As in reference 2 it can be shown from continuity considerations that if ψ is zero along the driving face of the blade (blade surface in the direction of rotation) the stream function ψ_t along the trailing face is constant and equal to

$$\psi_t = \varphi(\Delta\theta) \quad (18)$$

In equation (18) the channel flow coefficient φ is defined by

$$\varphi = \frac{W}{\rho_O a_{T^*} c_O} \quad (19)$$

where W is the flow rate through the channel and a_T is the channel flow area at the blade tip

$$a_T = r_T h_T(\Delta\theta) \quad (19a)$$

For incompressible flow

$$(\psi_1)_t = \frac{\psi_t}{M_T} = \frac{\varphi}{M_T} (\Delta\theta) \quad (20)$$

The Joukowski condition and other boundary conditions are discussed in reference 2.

NUMERICAL EXAMPLES

Solutions are presented for four flow rates through each of two centrifugal impellers with the same hub-shroud contours but with different blade spacings. The solutions are for incompressible flow on a surface of revolution generated by the mean streamline of an axial-symmetry solution.

Design and Operating Conditions

Impeller geometry. - The hub-shroud profile of the impellers is described in figure 7. The impeller blades are straight and thin, and for mathematical simplicity extend indefinitely far upstream parallel with the axis of the impeller. The diffuser is vaneless. Solutions were obtained for two blade spacings that, after accounting for the blade thickness, measured 14.67° and 32.80° about the axis.

Operating conditions. - The fluid was considered to be incompressible and nonviscous. The solutions were obtained on a flow surface of revolution generated by the mean (0.5) streamline of the axial-symmetry solution in figure 2 (the R,Z-coordinates of which streamline were obtained from results of reference 4 and are given in table I together with $\sin \alpha$ and H). Four solutions for different flow rates were obtained for each of the two blade spacings. At low flow rates an eddy (reference 2) exists on the driving face of the blade and at zero flow (closed throttle but impeller rotating) the eddy occupies the entire passage. As indicated in reference 2 the eddy flow, which consists of fluid that remains in the impeller and rotates relative to the impeller with an angular velocity equal and opposite to that of the impeller, results from the condition of absolute irrotational fluid motion. The four solutions for each blade spacing were obtained for the following flow conditions: (1) eddy flow (no through flow so that the eddy occupies entire channel), (2) zero eddy flow (through flow rate just sufficient to eliminate eddy), (3) half eddy flow (half of the through flow rate required to eliminate eddy), and (4) through flow rate used in axial-symmetry solution (fig. 2) of reference 4. These flow rates can be expressed by ratios of upstream axial velocity to impeller tip speed $(Q_Z/M_T)_U$. The through flow rate required to eliminate the eddy varies with the blade spacing so that the values of $(Q_Z/M_T)_U$ for the four flow conditions described are given for both blade spacings in the following table:

Blade spacing Flow condition $\Delta\theta$, deg	$\left(\frac{Q_Z}{M_T}\right)_U$	
	14.67	32.80
Eddy flow	0	0
One half eddy flow	.060	.105
Zero eddy flow	.120	.210
Flow rate of axial symmetry solution	.3429	.3429

The solutions for the various ratios of flow rate to impeller tip speed were obtained by superposition of the eddy flow solution (rotating impeller with no through flow) with various percentages of the through flow solution (flow through nonrotating impeller).

Results

The results of the numerical examples are presented in figures 8 to 11. The results are plotted on the surface of revolution between two impeller blades. The ξ, η coordinate system is shown on the surface of revolution. The relation between $\xi(\Delta\theta)$ and the specified cylindrical coordinates R and Z along the surface of revolution was obtained from a numerical integration of equation (14a) and is given in table I. From equation (14b) η is related to θ by

$$\eta = \frac{\theta}{\Delta\theta}$$

Streamlines. - The streamline patterns on the surface of revolution are shown in figures 8 and 9 for the 32.80° and the 14.67° angular blade spacings, respectively. For each blade spacing the streamlines are given for the four specified flow rates. The impeller rotates in the clockwise direction so that the driving face of a blade is on the left of the channel and the trailing face on the right. Except for the complete eddy flow solutions (figs. 8(a) and 9(a)) the streamlines are designated by a stream function ratio $\psi_i/(\psi_i)_t$ such that the value of this ratio indicates the percentage of total channel flow between the streamline and the driving face of the blade. (For the complete eddy flow solutions the stream function ratio $\psi_i/(\psi_i)_{\min}$ indicates the percentage of total flow rate circulating within the channel between the streamline and the nearest blade.) At each radius the spacing of the streamline is indicative of the relative velocity, with close spacing indicating high

velocities and wide spacing indicating low velocities. Thus, the velocities are higher on the trailing face of the blade than on the driving face, except at the blade tip where the velocities are equal on both faces and except for the complete eddy flow solutions (figs. 8(a) and 9(a)) where the velocities are equal on both faces at equal radii.

As indicated in the figures the fluid within the eddy remains in the impeller and rotates in the opposite direction to that of the impeller so that the velocities are inward along the driving face. (Also see reference 2, for example.) The eddy flow, which results from the condition of absolute irrotational motion, is associated with changes in radius along the rotating flow surface and disappears as the upstream surface becomes cylindrical (constant radius). This situation is most clearly evident in the solutions for no through flow (figs. 8(a) and 9(a)). Thus, for quasi-three-dimensional solutions the eddy flow disappears when the surfaces of revolution become cylindrical. (This condition is commonly assumed when two-dimensional cascade data are applied to the design of axial-flow turbomachines.) For rigorous three-dimensional solutions the eddy continues to exist but its plane is normal to the axis of the turbomachine and results only in a distortion of the initially cylindrical surface. If this distortion is neglected by assuming the flow is constrained to surfaces of revolution, the eddy disappears on cylindrical surfaces.

In the solutions for no through flow (figs. 8(a) and 9(a)) the greater magnitude of $(\psi_1)_{\min}$ for $\Delta\theta$ equal to 32.80° than for $\Delta\theta$ equal to 14.67° indicates that the magnitude of the eddy flow rate increases with increasing blade spacing.

Relative velocity components. - Lines of constant relative velocity components are shown in figures 10 and 11 for the 32.80° and 14.67° angular blade spacings, respectively. The meridional and relative tangential velocity components $\left(\frac{Q_M}{M_T} \text{ and } \frac{Q_\theta}{M_T}\right)$ are plotted and only the solutions for the eddy flow are considered. (For solutions with through flow, $\frac{Q_\theta}{M_T}$ remains the same and $\frac{Q_M}{M_T}$ is increased an amount, given in table I, that is proportional to $\left(\frac{Q_Z}{M_T}\right)_U$ and is a function of $\xi(\Delta\theta)$ only.)

Lines of constant relative tangential velocity $\frac{Q_\theta}{M_T}$ are plotted in figures 10(a) and 11(a). The values of $\frac{Q_\theta}{M_T}$ near the impeller tip are

negative so that the slip factor μ (defined as the ratio of the average absolute tangential velocity at the impeller tip to the impeller tip speed) is less than 1.0. The resulting slip factors for the two blade spacings are

Blade spacing $\Delta\theta$ (deg)	Slip factor μ
14.67	0.9111
32.80	.8142

Because $\frac{Q_\theta}{M_T}$ is unaffected by the through flow the values of μ are independent of the flow rate (also see reference 6). The values of $\frac{Q_\theta}{M_T}$ at lower values of R upstream of the impeller tip approach a maximum positive value and then decrease to zero as the surface of revolution becomes cylindrical. It is noted that the maximum positive value of $\frac{Q_\theta}{M_T}$ is considerably larger for the wider blade spacing.

Lines of constant meridional velocity $\frac{Q_M}{M_T}$ are plotted in figures 10(b) and 11(b). The values of $\frac{Q_M}{M_T}$ are negative along the driving face and positive along the trailing face with zero values along the center line of the channel between blades. The maximum values of $\frac{Q_M}{M_T}$ occur on the blade surfaces near the impeller tip and as the radius decreases $\frac{Q_M}{M_T}$ decreases and approaches zero as the upstream surface of revolution becomes cylindrical. It is noted, as for $\frac{Q_\theta}{M_T}$, that as the blade spacing increases the magnitude of $\frac{Q_M}{M_T}$ increases.

CORRELATION OF RESULTS

The relaxation solutions presented in this report required considerable labor and it is therefore desirable to have a more rapid method of analysis to serve as a useful engineering tool. The correlation equations to be presented in this section have been developed for this objective. These equations are limited to impellers with straight blades on arbitrary surfaces of revolution, but other less accurate methods of analysis have been developed for blades with arbitrary shape (reference 7, for example). The correlation equations to be developed are an extension of the correlation equations developed for straight blades on conic flow surfaces of revolution in reference 6. This extension enables the correlation equations to apply to arbitrary surfaces of revolution. In this report, as well as in reference 6, the correlation equations are developed to predict the distribution of the relative velocity components Q_θ and Q_M and the stream function ψ throughout the impeller passage. The correlation equations are developed from the fundamental conditions of continuity and absolute irrotational motion and from certain observed results of the relaxation solutions. These correlation equations predict flow conditions in straight-bladed impellers with any tip speed, flow rate, area variation, blade spacing, and for any flow surface of revolution. The correlation equations determine these flow conditions from various parameters that describe the design and operating conditions of the impeller and from tabulated values of any known "standard" solution (such as that given in reference 6).

In the correlation equations of this report, and of reference 6, the standard conditions (obtained from any known solution, reference 6, for example) and the nonstandard conditions (being investigated by the correlation equations) are evaluated at the same values of ξ and η . The effect of the shape of the surface of revolution on the fluid properties at a given point (ξ, η) on the surface of revolution is determined by the effect of the shape on $\sin \alpha$, which term appears in the correlation equations, and by the effect of the shape on ξ , which quantity is related to $\sin \alpha$ by equation (14a).

Compressible flow. - In the previous development of correlation equations the local velocity was found to be, in effect, made up of the average value of Q_M at the given radius and superimposed velocity components caused by the rotation of the channel. The superimposed velocity components were sufficiently small not to be greatly affected by compressibility, which was only considered to affect the average value of Q_M .

Because this effect on Q_M is easily incorporated, the correlation equations in this report are developed for compressible as well as incompressible flow.

Assume that the Q_θ component of the relative velocity is correlated by

$$Q_\theta' = A(Q_\theta)_s \quad (21)$$

where the superscript prime indicates approximate values determined by the correlation equations, where the subscript s indicates standard values (given in tables of reference 6, for example), and where

$$A = \frac{M_T (\Delta\theta) \sin \alpha}{[M_T (\Delta\theta) \sin \alpha]_s} \quad (22)$$

For constant α equation (21) is identical to the corresponding correlation equation of reference 6. (Note the different definition of $\Delta\theta$ in reference 6.)

From equation (21) and using the identical procedure described in reference 6, the correlation equation for Q_M becomes

$$Q_M' = (Q_M)_{av} + A \left[Q_M - (Q_M)_{av} \right]_s + A(2\eta - 1) \left\{ \frac{(Q_\theta)_s}{2} \left[(\Delta\theta) \sin \alpha - (\Delta\theta)_s \sin \alpha_s \right] + (R - R_s) (M_T \Delta\theta)_s \sin \alpha_s \right\} \quad (23)$$

where R is a known function of ξ and where from one-dimensional continuity considerations (reference 6)

$$(Q_M)_{av} = \frac{\varphi}{\frac{\rho_{av}}{\rho_o} RH} \quad (24)$$

In equation (24) the average density ratio ρ_{av}/ρ_o is obtained from equation (9) by assuming that for straight blades the relative tangential velocity is zero and the meridional velocity is equal to its average value so that

$$Q^2 \approx (Q_M)_{av}^2$$

Likewise the correlation equation for the stream function ψ becomes

$$\frac{\psi'}{\psi_t} = \eta + \frac{A}{(Q_M)_{av}} \left(\left[(Q_M)_{av} \left(\frac{\psi}{\psi_t} - \eta \right) \right]_s + (\eta - 1) \eta \left\{ \frac{(Q_\theta)_s}{2} \left[(\Delta\theta) \sin \alpha - (\Delta\theta)_s \sin \alpha_s \right] + (R - R_s) (M_T \Delta\theta)_s \sin \alpha_s \right\} \right) \quad (25)$$

For a complete eddy flow (no through flow) ψ_t and $(Q_M)_{av}$ are zero so that equation (25) becomes indeterminate. If, however, both sides of equation (25) are multiplied by

$$\psi_t = \frac{\rho_{av}}{\rho_o} (Q_M)_{av} HR (\Delta\theta)$$

which equality is obtained from equations (18) and (24), equation (25) can be evaluated directly for ψ' .

Incompressible flow. - For incompressible flow the stagnation speed of sound can, as before, be eliminated from consideration by expressing Q and ψ as ratios of M_T . Thus for incompressible flow the correlation equations become

$$\left(\frac{Q_\theta}{M_T} \right)' = A^* \left(\frac{Q_\theta}{M_T} \right)_s \quad (21a)$$

where

$$A^* = \frac{(\Delta\theta) \sin \alpha}{[(\Delta\theta) \sin \alpha]_s} \quad (22a)$$

$$\begin{aligned} \left(\frac{Q_M}{M_T} \right)' &= \left[\frac{(Q_M)_{av}}{M_T} \right] + A^* \left\{ \left(\frac{Q_M}{M_T} \right) - \left[\frac{(Q_M)_{av}}{M_T} \right] \right\}_s + \\ &A^* (2\eta - 1) \left\{ \frac{1}{2} \left(\frac{Q_\theta}{M_T} \right)_s \left[(\Delta\theta) \sin \alpha - (\Delta\theta)_s \sin \alpha_s \right] + \right. \\ &\quad \left. (R - R_s) (\Delta\theta)_s \sin \alpha_s \right\} \end{aligned} \quad (23a)$$

and

$$\frac{\psi_1'}{(\psi_1)_t} = \eta + \frac{A^*}{\left[\frac{(Q_M)_{av}}{M_T}\right]} \left(\left[\frac{(Q_M)_{av}}{M_T} \left(\frac{\psi}{\psi_t} - \eta \right) \right]_S + \right. \\ \left. (\eta - 1) \eta \left\{ \frac{1}{2} \left[\frac{(Q_\theta)}{M_T} \right]_S \left[(\Delta\theta) \sin \alpha - (\Delta\theta)_S \sin \alpha_S \right] + \right. \right. \\ \left. \left. (R - R_S) (\Delta\theta)_S \sin \alpha_S \right\} \right) \quad (25a)$$

Representative values of $\left(\frac{Q_\theta}{M_T}\right)$, $\left(\frac{Q_M}{M_T}\right)$, and $\frac{\psi_1}{(\psi_1)_t}$ obtained by the relaxation solutions of this report are compared in figures 12 to 14 with the corresponding values given by the correlation equations [(21a), (23a) and (25a)] using the standard solution given in reference 6. Perfect agreement corresponds to the 45° straight line, and it is seen that the correlation equations are accurate.

Effect of flow surface shape. - The correlation equation (23a) has been used to compute the velocity distribution on the blade surfaces for incompressible flow in impellers with straight blades, with constant flow area along the flow surface, and with various shapes of flow surfaces of revolution. These flow surfaces are described by the shape of their generating lines (meridional streamlines) in the RZ-plane. In order to demonstrate the effect of flow surface shape, calculations have been carried out for generating lines that are described by the equation

$$R = \frac{1}{2} \left[(2Z - 1)^n + 1 \right] \quad (26)$$

The family of generating lines is given by various values for the parameter n , and as indicated in figure 15, the surfaces in all cases start at a radius R of 0.5 (impeller inlet) and end at a radius R of 1.0 (impeller tip).

The resulting velocity distributions on the blade surfaces are plotted in figure 16. As the value of n decreases, the difference in velocity on the two blade surfaces toward the impeller tip decreases and in the limit as n approaches zero the velocities become equal on both

surfaces. At this limiting value of n equal zero the flow is axial (see generating line for n equal to zero in fig. 15) and the velocities on both blade surfaces are equal to the average velocity $\left(\frac{Q_M}{M_T}\right)_{av}$, which for these examples is constant because of the constant prescribed flow area.

As the value of n increases the difference in velocity on the two blade surfaces toward the impeller tip increases and in the limit as n approaches infinity this difference approaches that for a radial flow impeller (see generating line for n equal to infinity in figure 15).

If the velocity distribution curves in figure 16 were extrapolated to lower values of R , the curves would cross because, as indicated in figure 15, the flow surfaces that are more nearly radial near the impeller tip are more nearly axial near the impeller inlet, and vice versa.

SUMMARY OF RESULTS

A general method of analysis is developed for steady, two-dimensional, compressible, nonviscous, irrotational flow between arbitrary blade shapes on arbitrary flow surfaces of revolution in turbomachines. Incompressible solutions are presented for four flow rates through each of two centrifugal impellers with the same hub-shroud contours but with different blade spacings. In addition, correlation equations are developed whereby the velocity components and the stream function distribution can be predicted for compressible or incompressible flow in straight-bladed impellers only, with any tip speed, flow rate, area variation, blade spacing, and for any flow surface of revolution.

Lewis Flight Propulsion Laboratory
National Advisory Committee for Aeronautics
Cleveland, Ohio, December 23, 1951

APPENDIX

SYMBOLS

The following symbols are used in this report:

A	parameter, equation (22)
A^*	parameter, equation (22a)
a_T	flow area at channel tip, equation (19a)
c_o	stagnation speed of sound upstream of turbomachine, equation (1)
g	gravitational acceleration
H	height ratio, equation (10)
h	spacing between center lines of channels formed by streamlines adjacent to streamline that generates surface of revolution, figure 2
M_T	blade-tip Mach number, equation (2)
n	exponent, equation (26)
P	pressure ratio, equation (8)
p	static pressure
Q	relative velocity expressed as ratio of c_o
Q_M	meridional component of Q , equation (3)
Q_R, Q_θ, Q_Z	components of Q in R , θ , and Z directions, respectively
R, θ, Z	cylindrical coordinates, dimensionless (linear coordinates R and Z expressed as ratios of r_T)
R^*	perfect gas constant
r_T	blade-tip radius
T	static temperature
W	total flow rate through channel (of height h) between two blades

α	angle, figures 3 and 4
Γ	dimensionless fluid circulation
γ	ratio of specific heats
η	transformed coordinate, equation (14b)
$\Delta\theta$	angular blade spacing about axis of turbomachine
λ	whirl ratio, equation (7)
μ	slip factor
ξ	transformed coordinate, equation (14a)
ρ	static weight density
φ	channel flow coefficient, equation (19)
ψ	stream function, equation (13)
ω	angular velocity of blade row

Subscripts:

av	average
i	incompressible
min	minimum
o	stagnation condition upstream of turbomachine
s	standard solution
T	blade tip
t	trailing face of blade
U	far upstream of turbomachine


Superscripts:

'	estimated by correlation equations
---	------------------------------------

REFERENCES

1. Wu, Chung-Hua and Brown, Curtis A.: Method of Analysis for Compressible Flow Past Arbitrary Turbomachine Blades on General Surface of Revolution. NACA TN 2407, 1951.
2. Stanitz, John D.: Two-Dimensional Compressible Flow in Turbomachines with Conic Flow Surfaces. NACA Rep. 935, 1949.
3. Hamrick, Joseph T., Ginsburg, Ambrose, and Osborn, Walter M.: Method of Analysis for Compressible Flow through Mixed-Flow Centrifugal Impellers of Arbitrary Design. NACA TN 2165, 1950.
4. Ellis, Gaylord O., Stanitz, John D., and Sheldrake, Leonard J.: Two Axial-Symmetry Solutions for Incompressible Flow Through a Centrifugal Compressor with and without Inducer Vanes. NACA TN 2464, 1951.
5. Southwell, R. V.: Relaxation Methods in Theoretical Physics. Clarendon Press (Oxford), 1946.
6. Stanitz, John D., and Ellis, Gaylord O.: Two-Dimensional Compressible Flow in Centrifugal Compressors with Straight Blades. NACA Rep. 954, 1950.
7. Stanitz, John D., and Prian, Vasily D.: A Rapid Approximate Method for Determining Velocity Distribution on Impeller Blades of Centrifugal Compressors. NACA TN 2421, 1951.

TABLE I - CHARACTERISTICS OF MEAN FLOW SURFACE OF
REVOLUTION USED IN NUMERICAL EXAMPLES



$\xi \cdot \Delta\theta$	R	Z	$\sin \alpha$	H	$\frac{Q_M/M_T}{(Q_Z/M_T)_U}$ (a)
-1.792	0.4915	-0.3394	0.0082	3.659	1.001
-1.664	.4920	- .2767	.0140	3.652	1.002
-1.536	.4930	- .2135	.0218	3.636	1.004
-1.408	.4950	- .1502	.0333	3.608	1.008
-1.280	.4978	- .0870	.0555	3.565	1.015
-1.152	.5021	- .0232	.0900	3.493	1.027
-1.024	.5096	.0411	.1422	3.364	1.050
- .896	.5212	.1058	.2222	3.160	1.093
- .768	.5408	.1710	.3550	2.858	1.165
- .640	.5722	.2348	.5372	2.544	1.237
- .512	.6205	.2933	.7312	2.236	1.298
- .384	.6890	.3408	.8888	1.901	1.374
- .256	.7770	.3737	.9678	1.542	1.502
- .128	.8803	.3931	.9913	1.239	1.651
0	1.0000	.4052	.9968	1.0000	1.800
.128	1.1368	.4120	.9996	.8700	1.820
.256	1.2919	.4127	1.0000	.8664	1.608

^aValues of $(Q_Z/M_T)_U$ for flow rates used in numerical examples of this report are given in the text under Operating conditions.

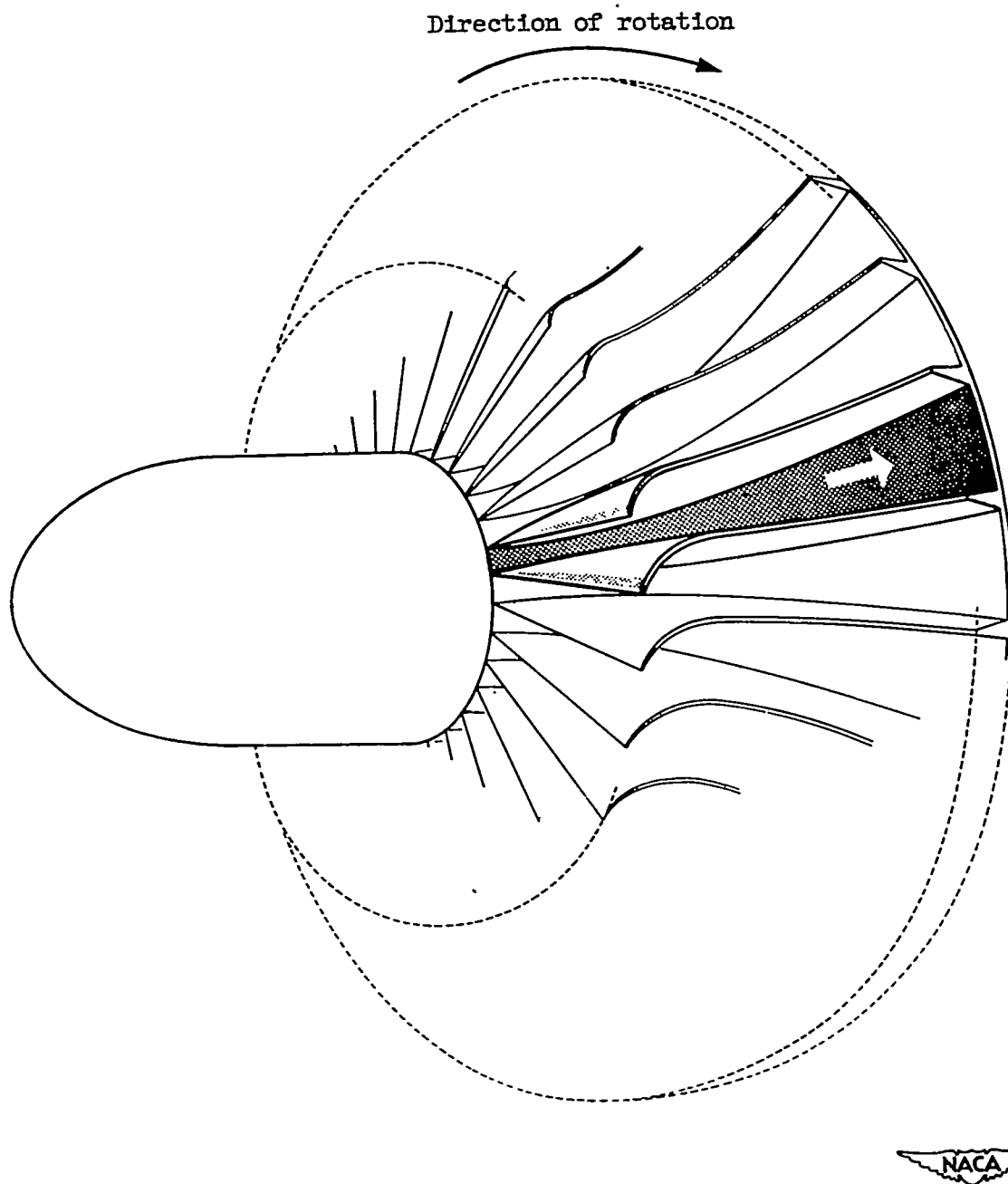


Figure 1. - Channel between blades of typical high-solidity blade row.

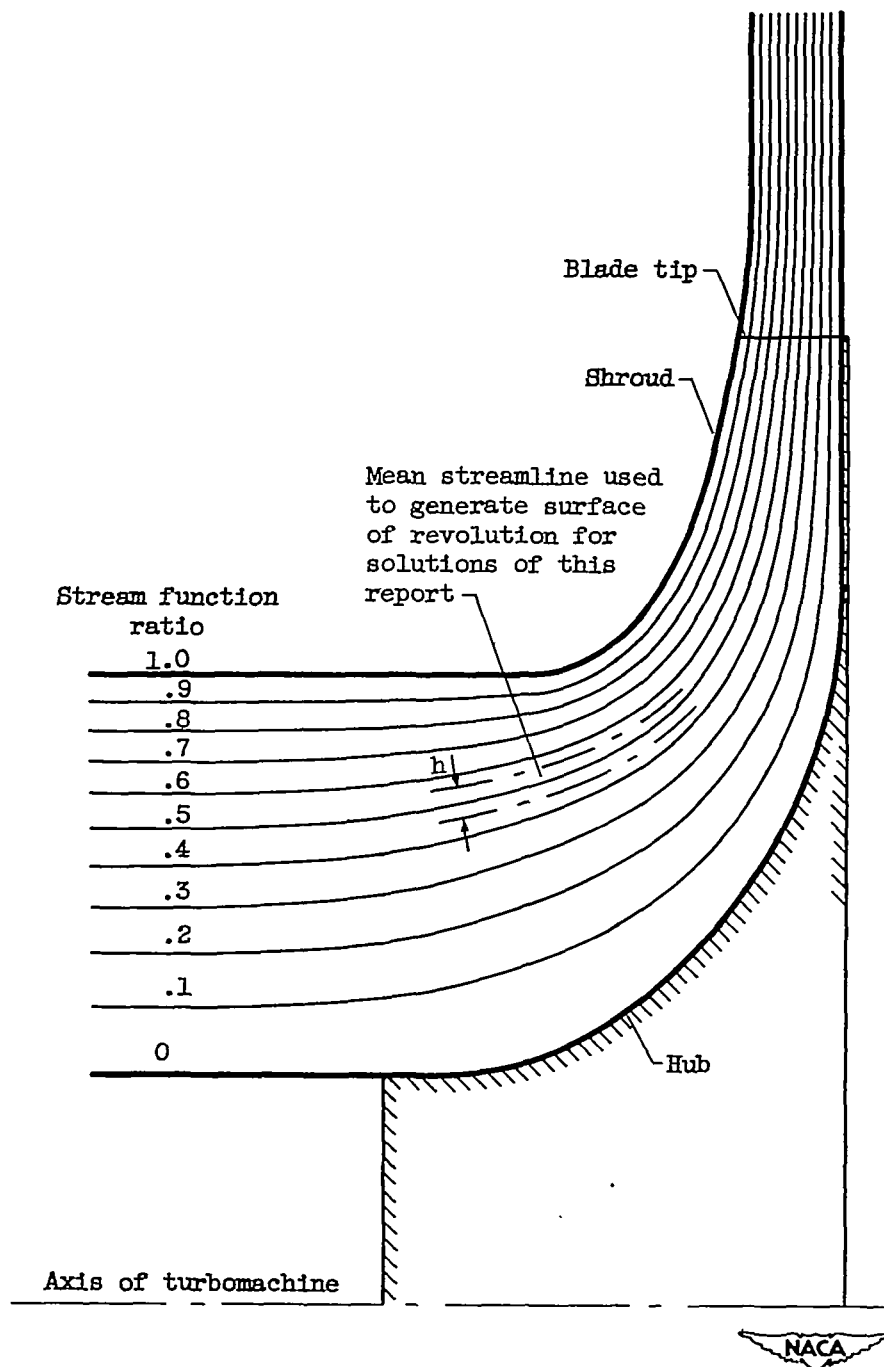


Figure 2. - Streamlines in meridional plane for axial-symmetry solution of channel described in figure 7. Streamline designation indicates percentage of flow through channel between streamline and hub. Incompressible flow; Q_Z/M_T equal to 0.3429 far upstream (reference 4).

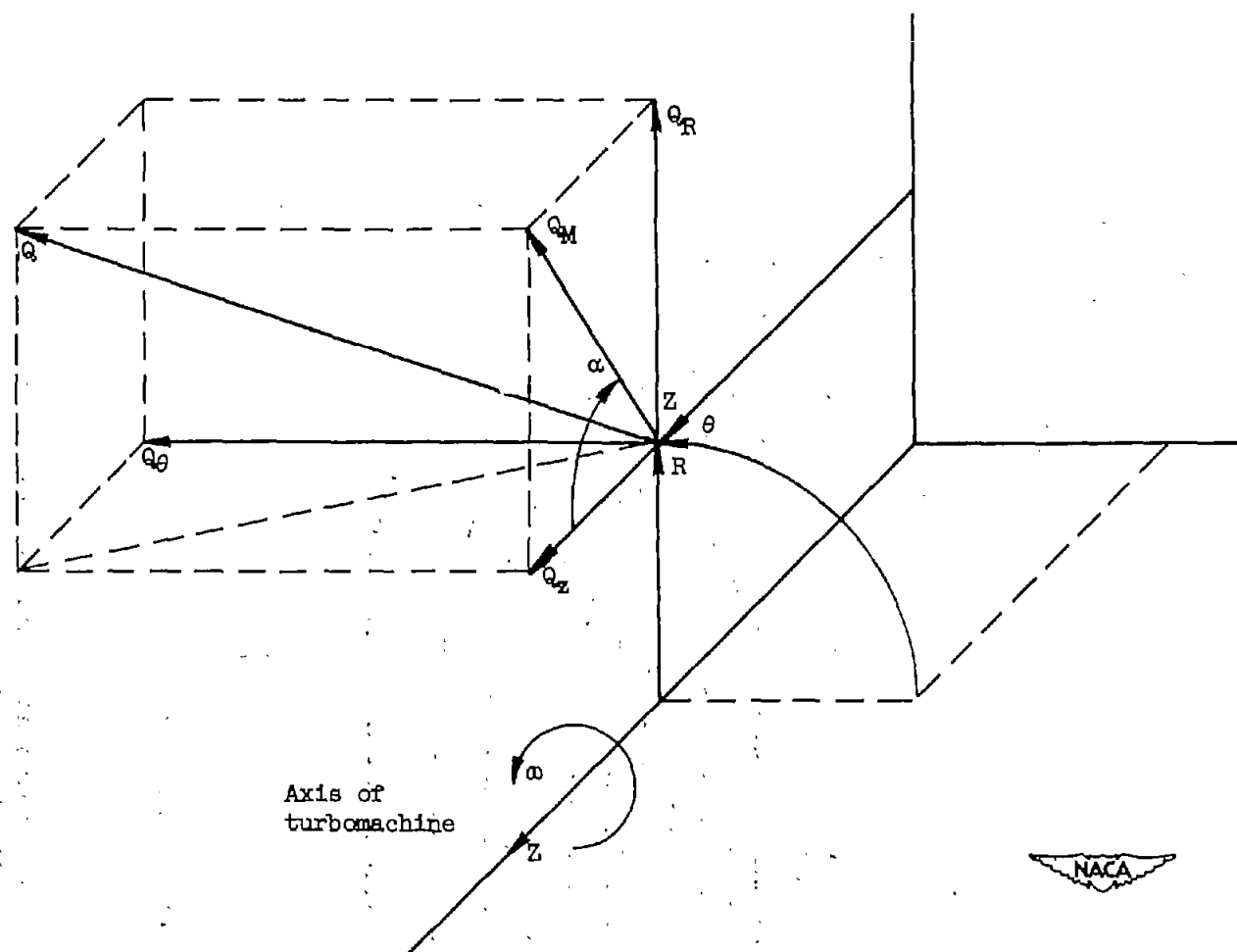


Figure 3. - Cylindrical coordinates and velocity components relative to rotating blade row. All quantities are dimensionless. Linear coordinates are measured in units of blade tip radius; velocity components are measured in units of stagnation speed of sound upstream of blade row.



2466

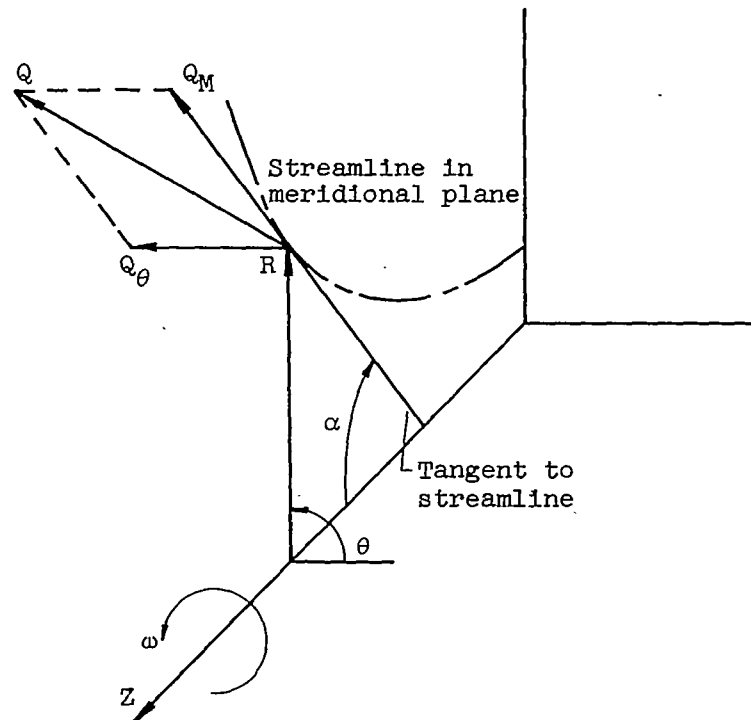


Figure 4. - Coordinates, velocities, and so forth at point on streamline in meridional plane (axial-symmetry solution).

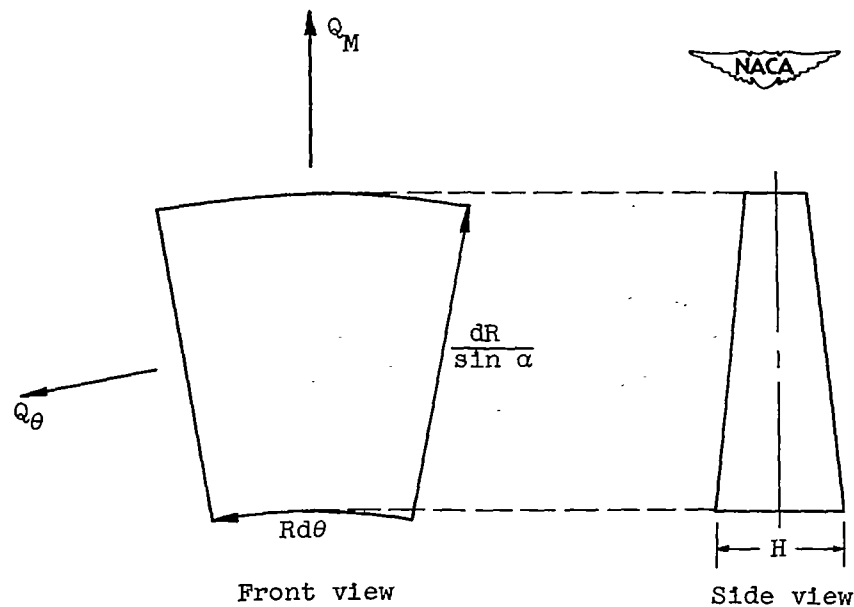


Figure 5. - Fluid particle on developed surface of cone at point that is tangent to flow surface of revolution.

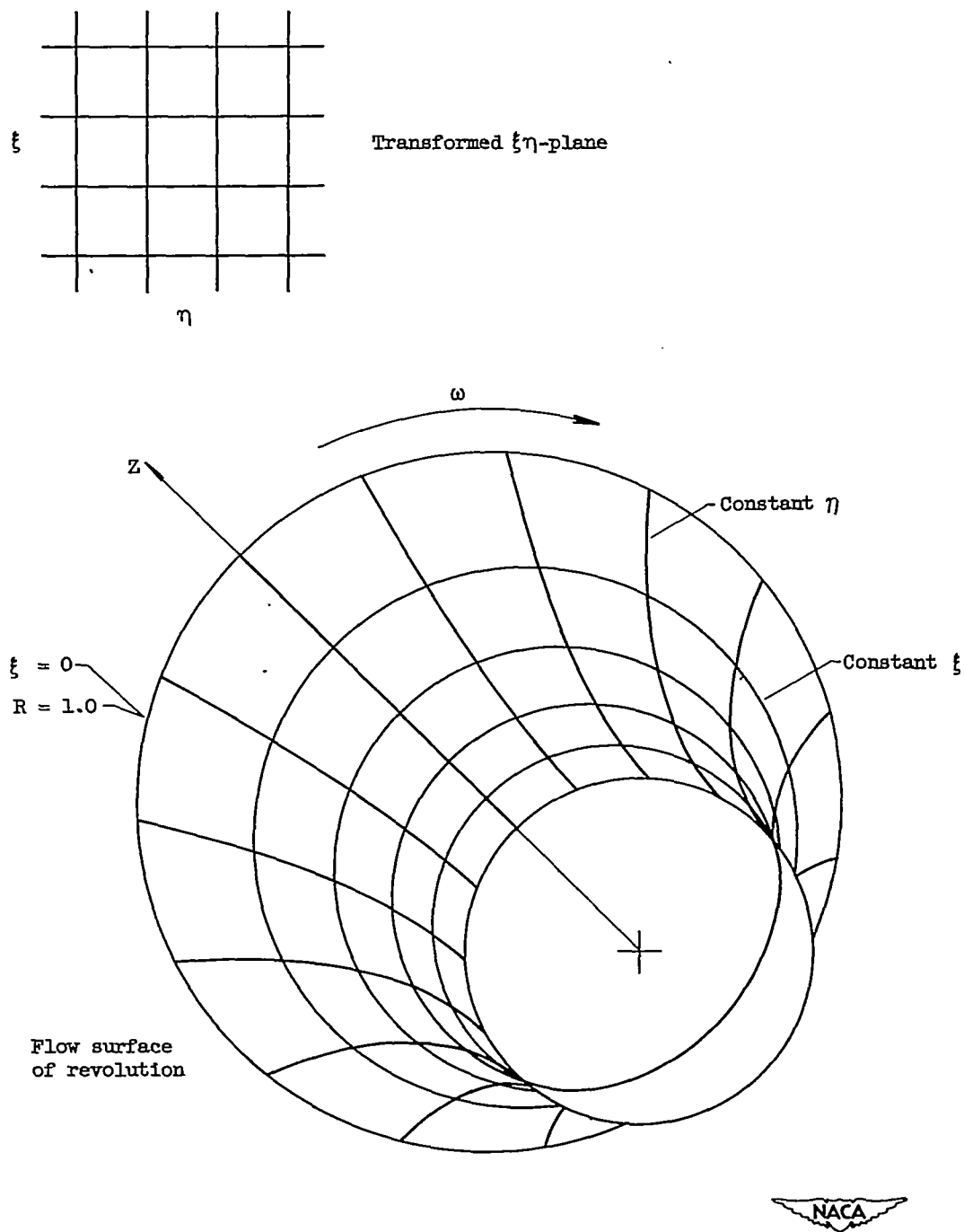


Figure 6. - Lines of constant ξ and η (coordinates of transformed $\xi\eta$ -plane) on flow surface of revolution.

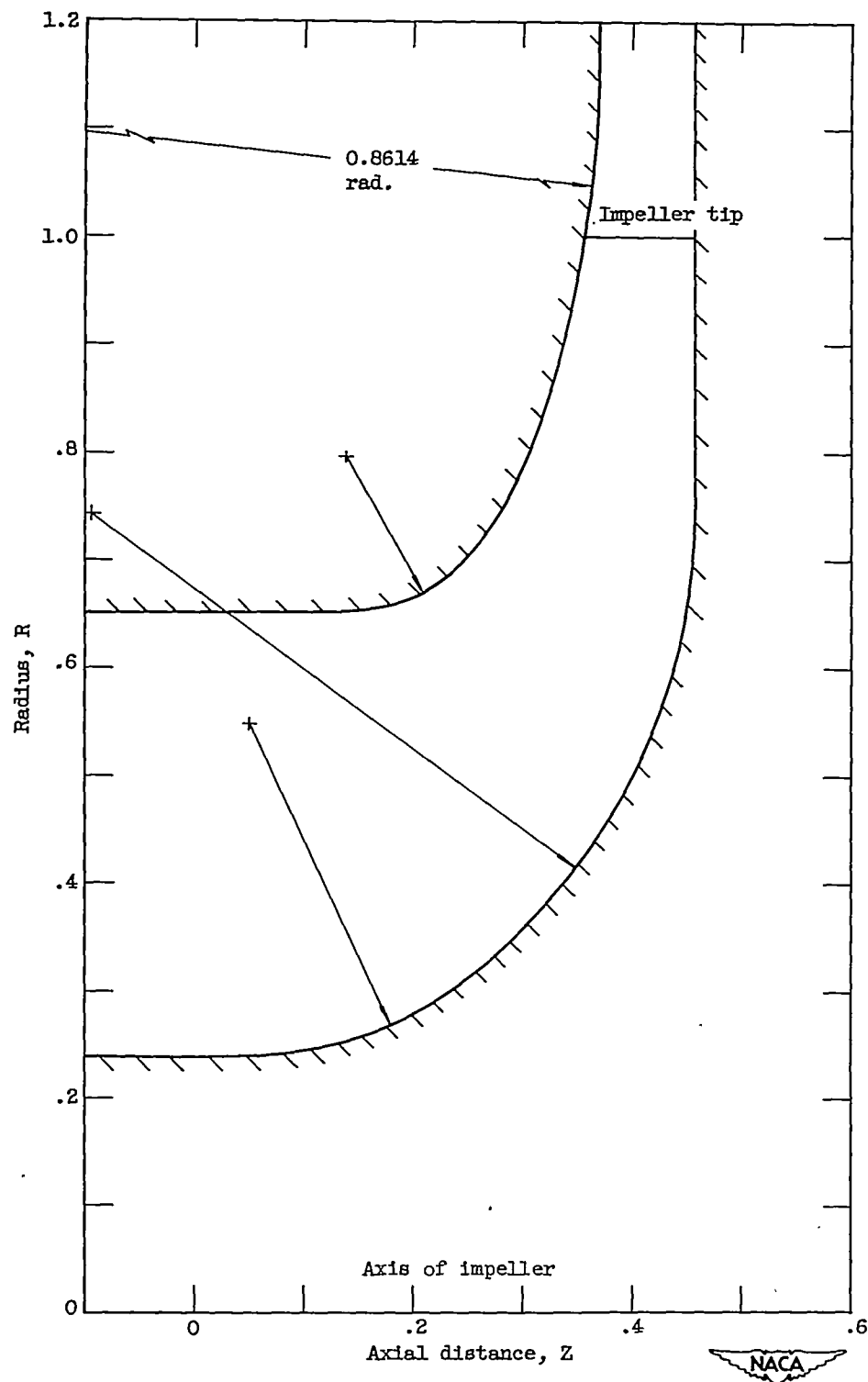
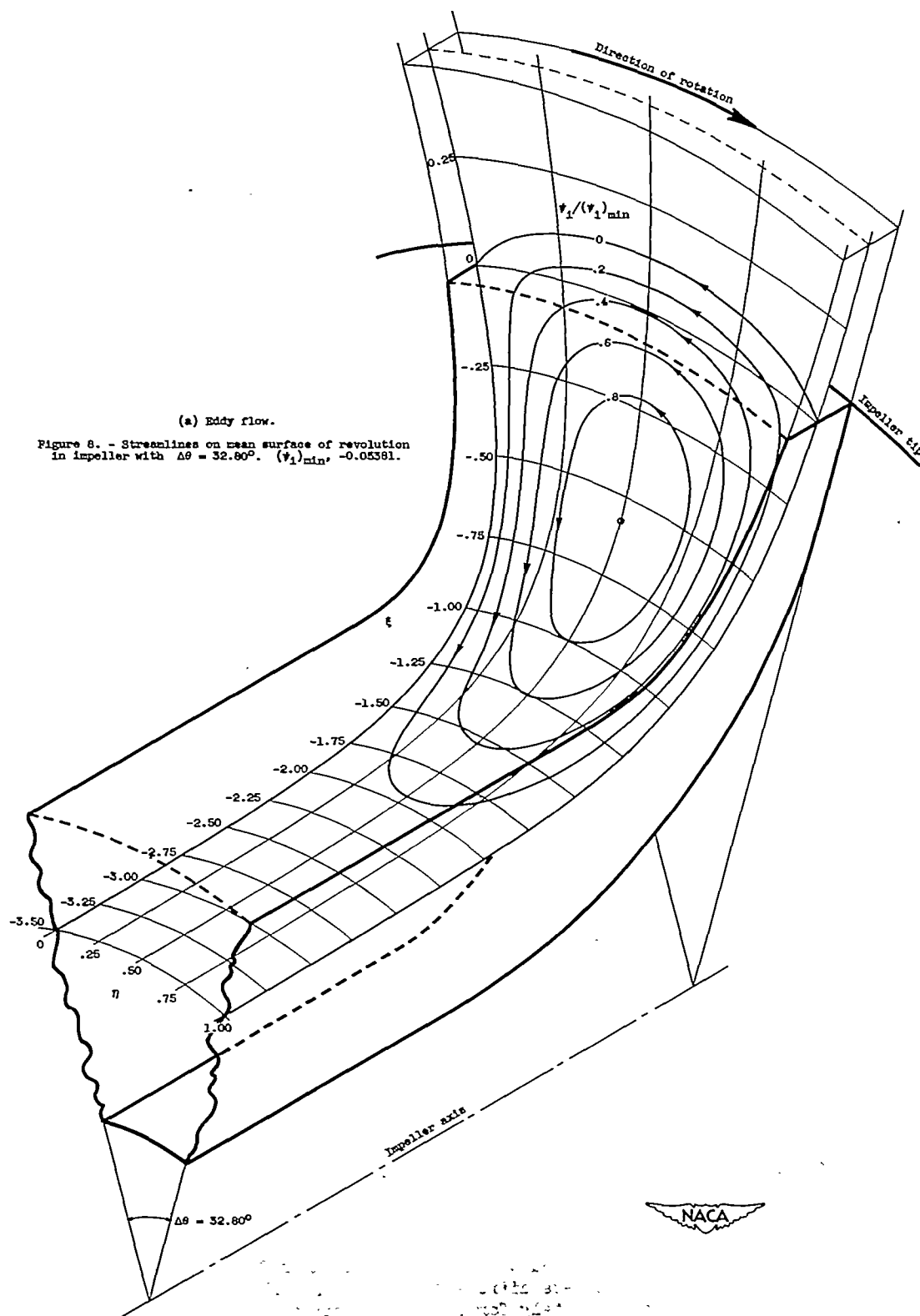
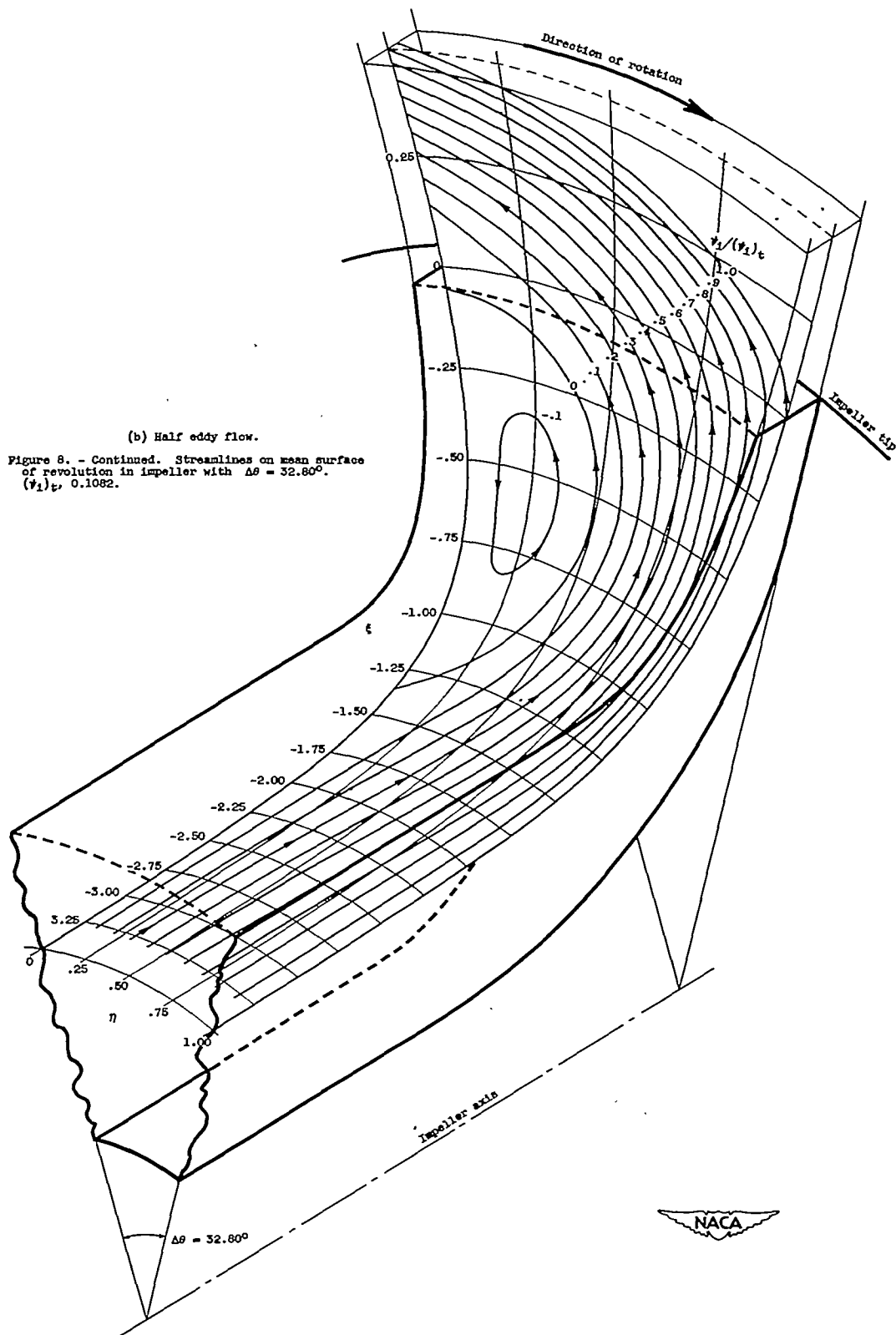
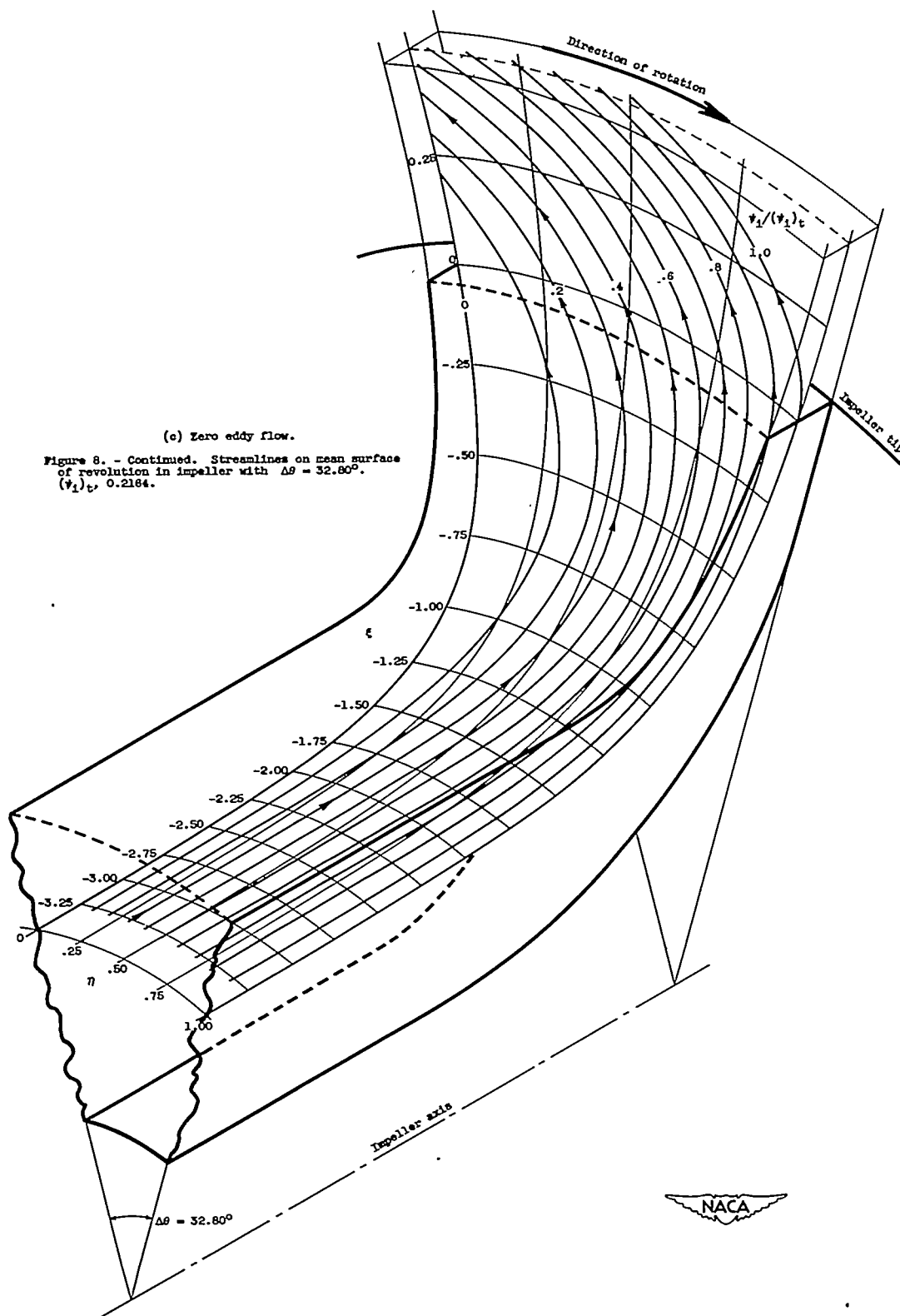


Figure 7. - Hub-shroud dimensions of impeller for numerical examples. Vaneless diffuser; straight impeller blades extended indefinitely far upstream parallel with axis of impeller.

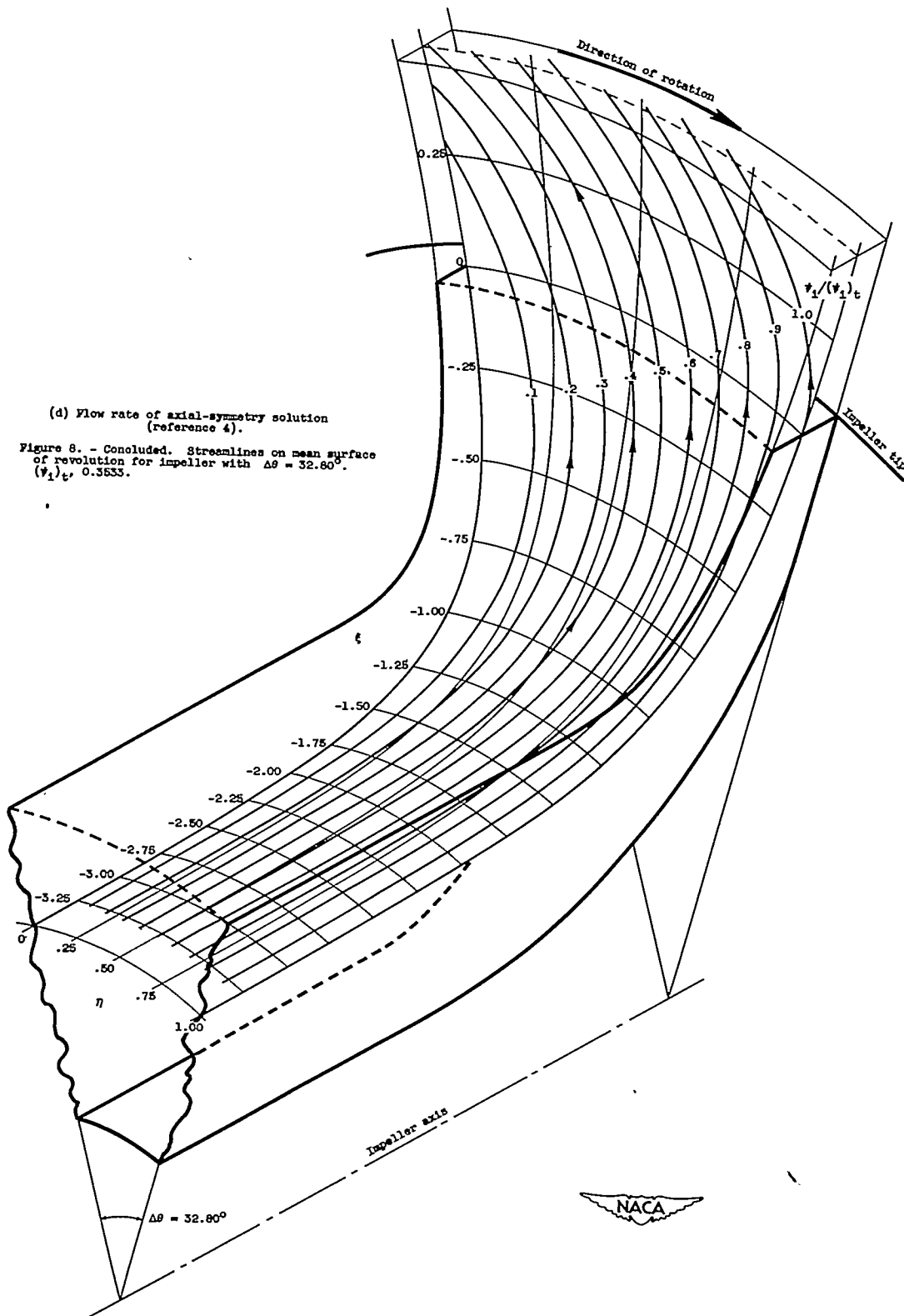


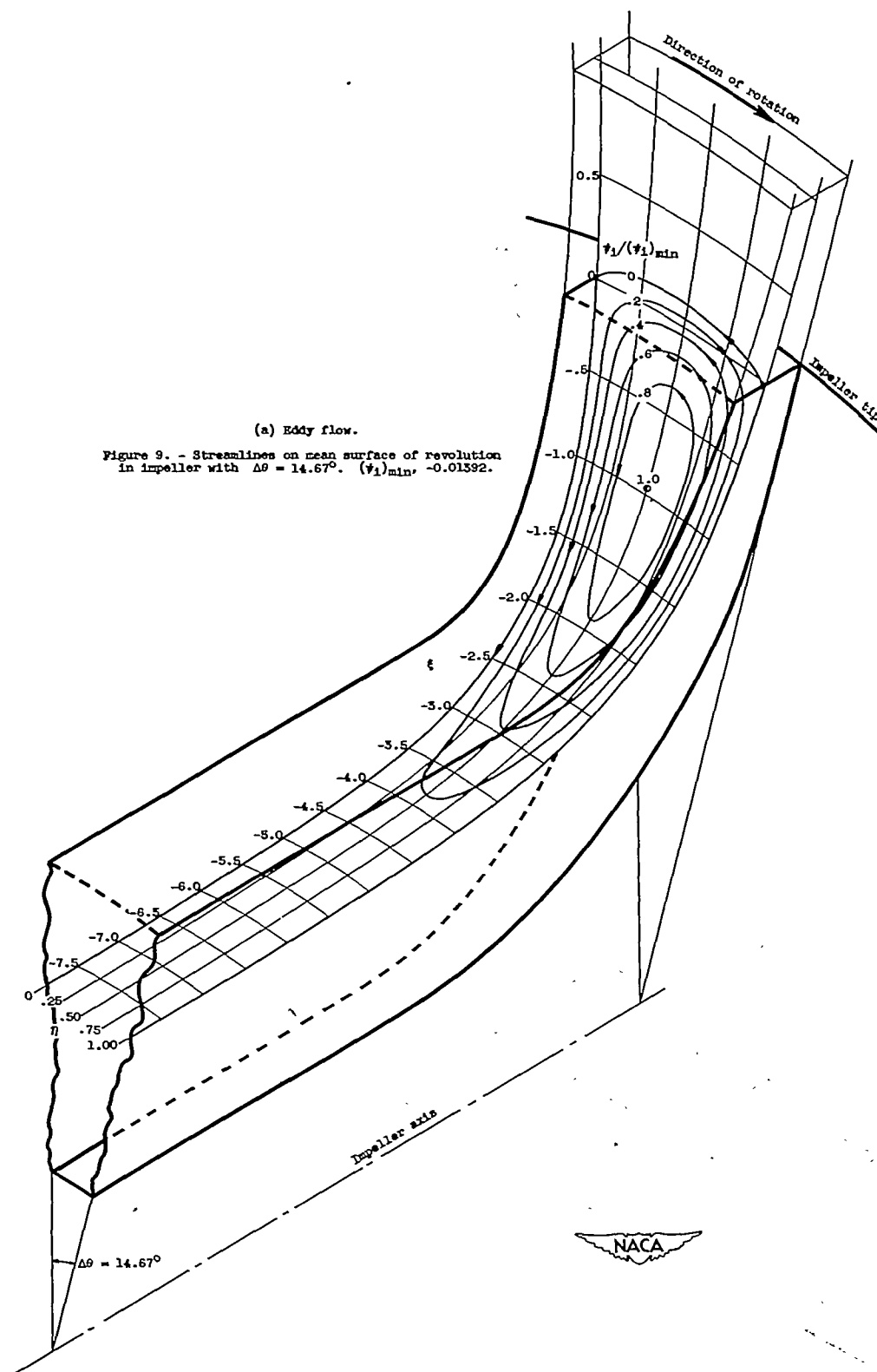
2466



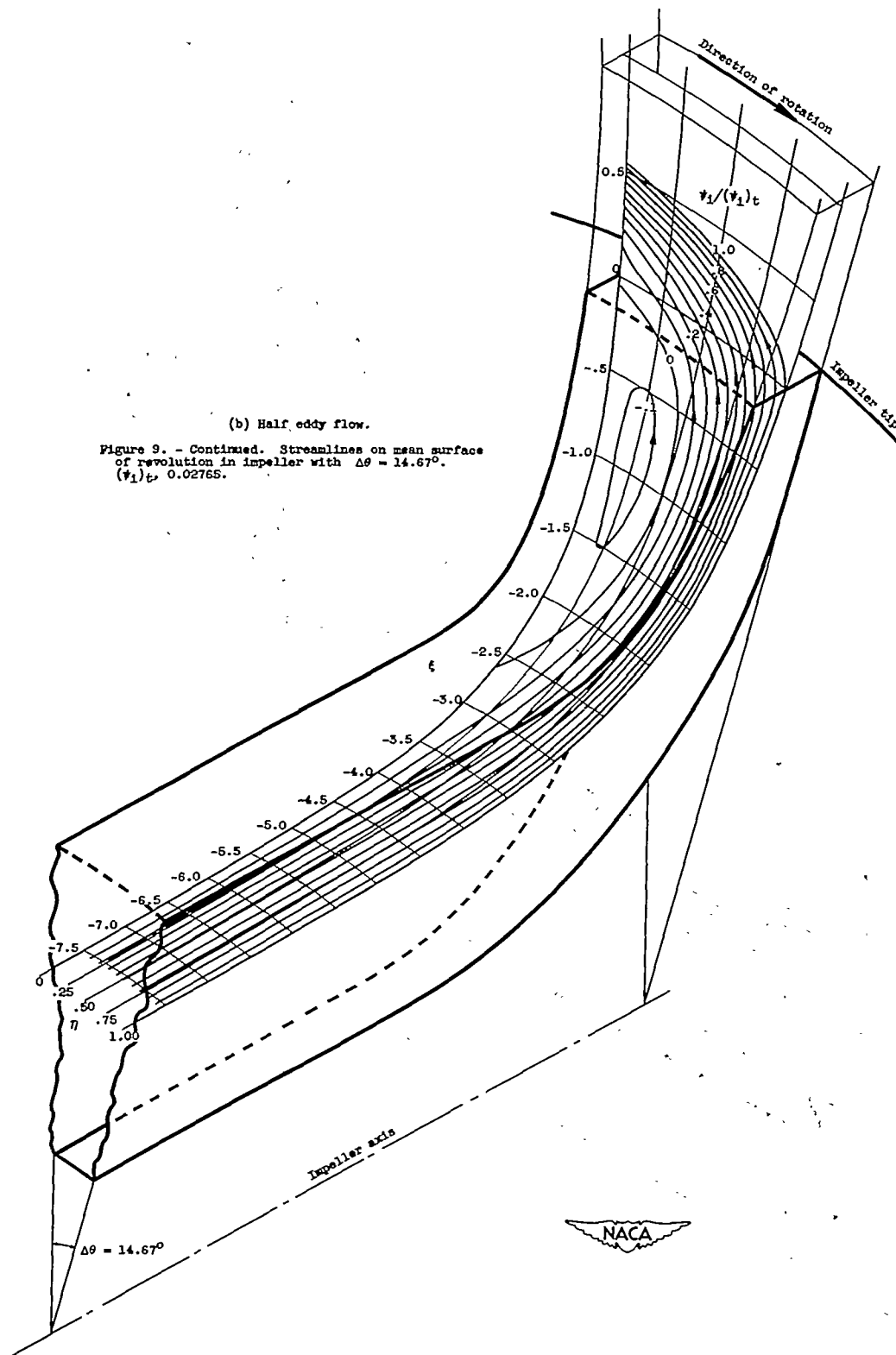


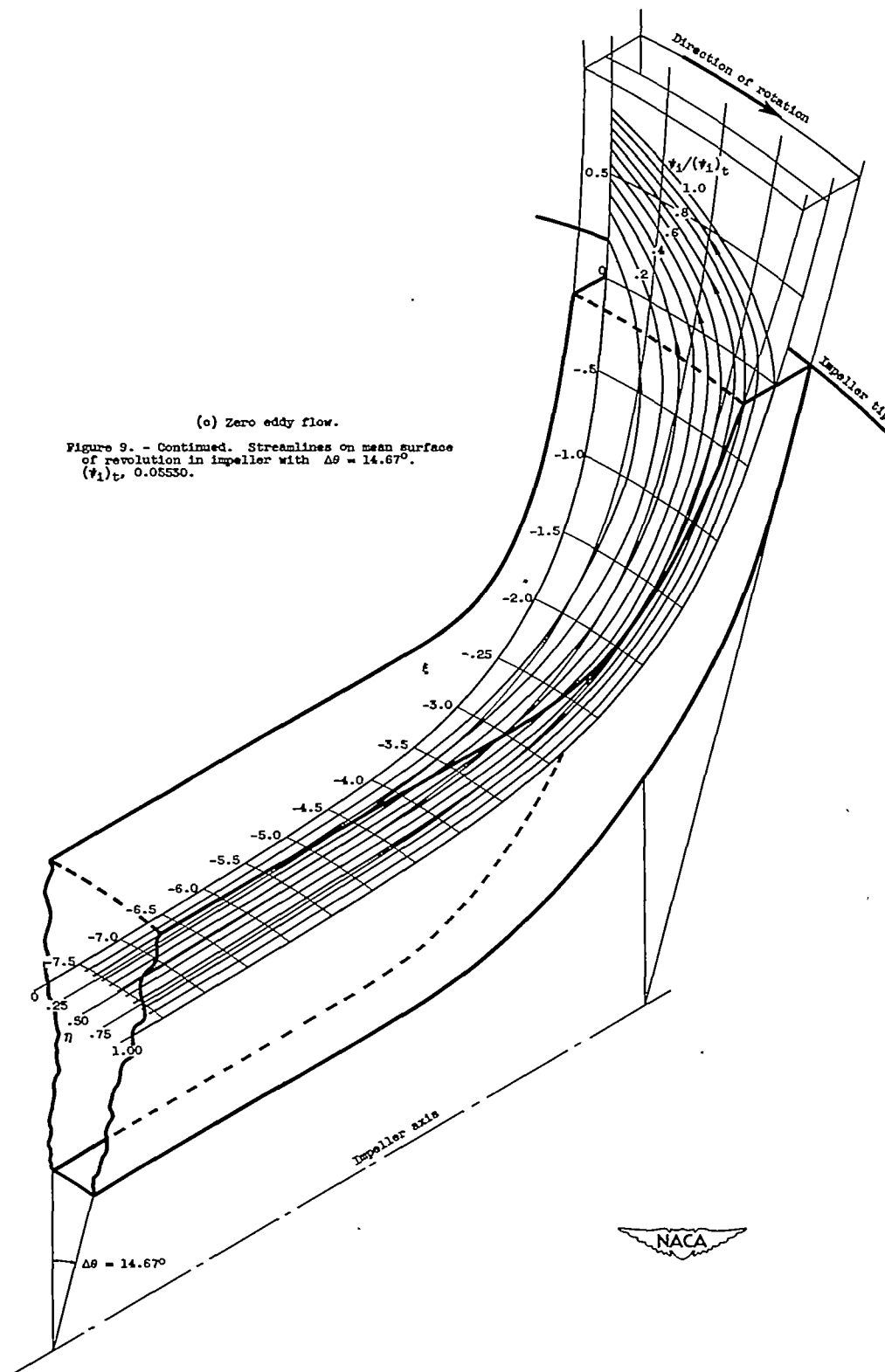
2466



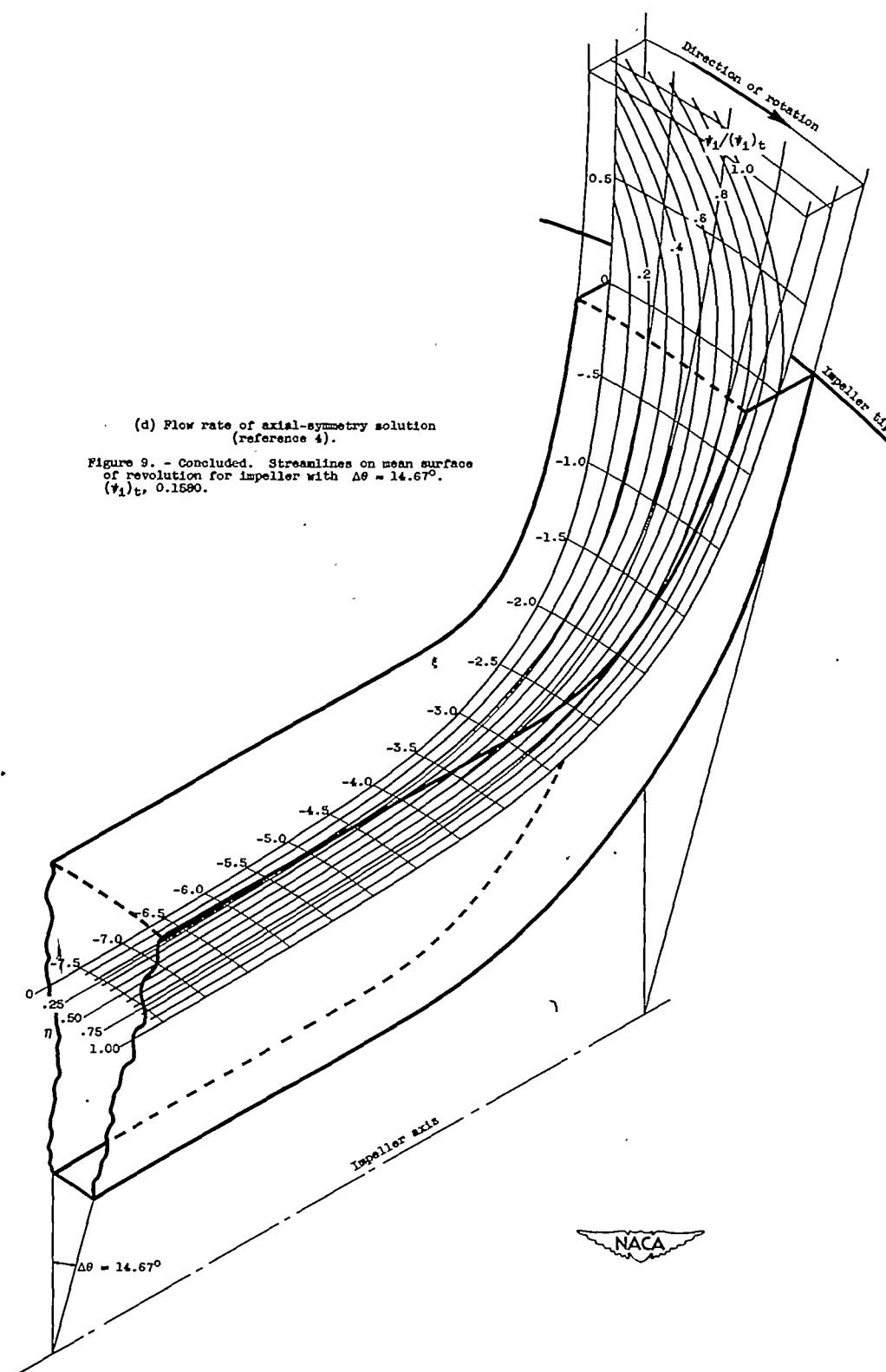


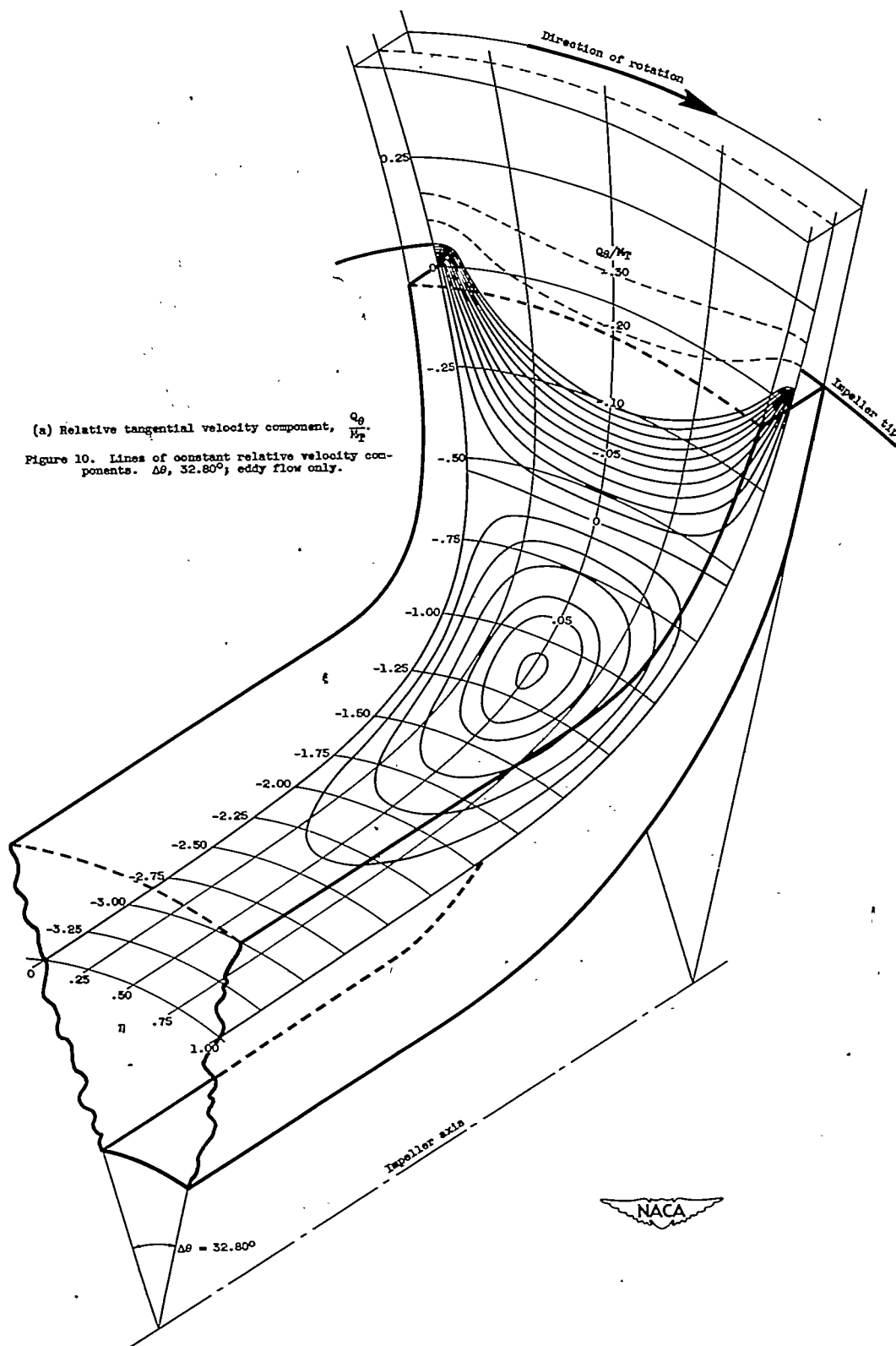
2466



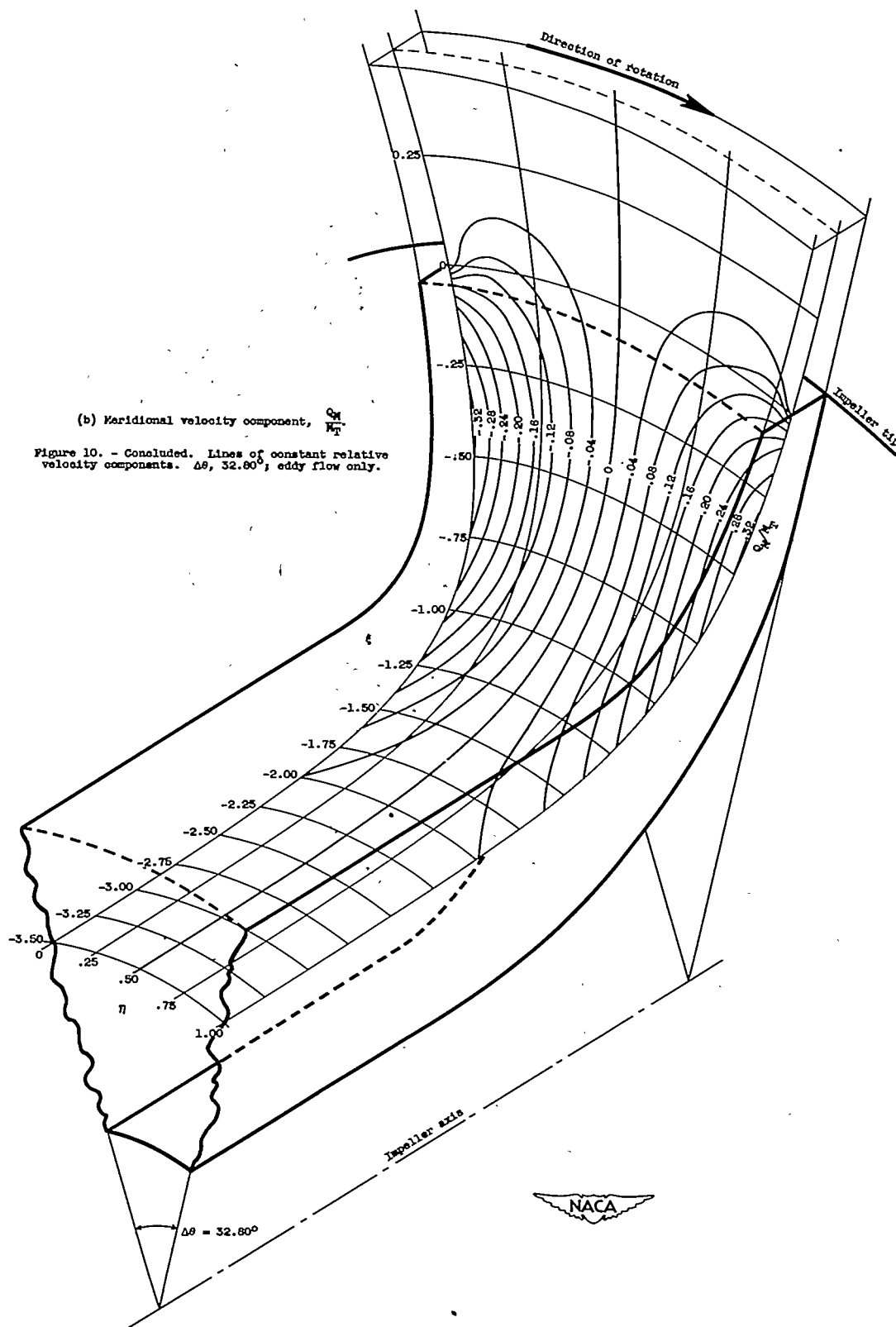


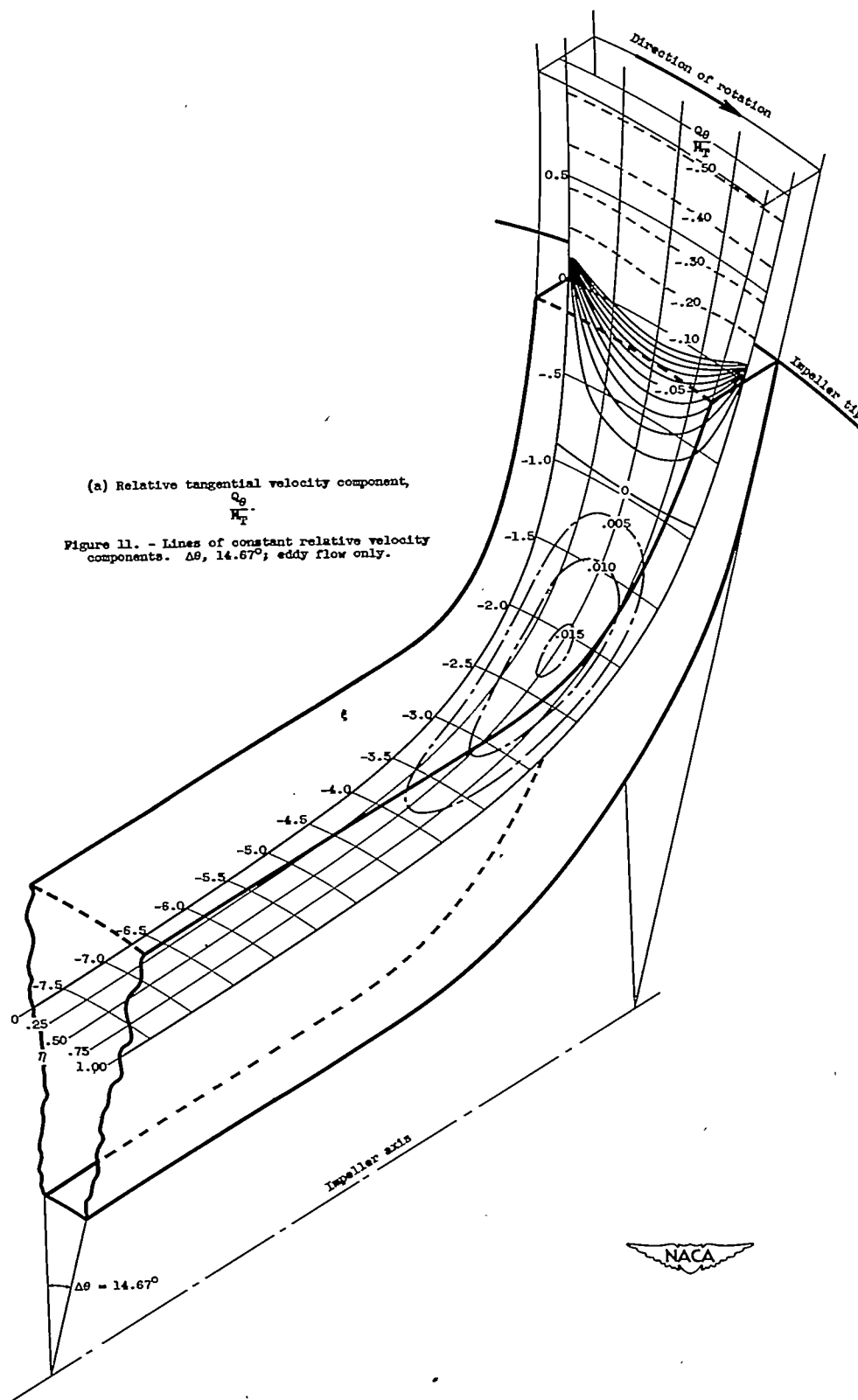
2466



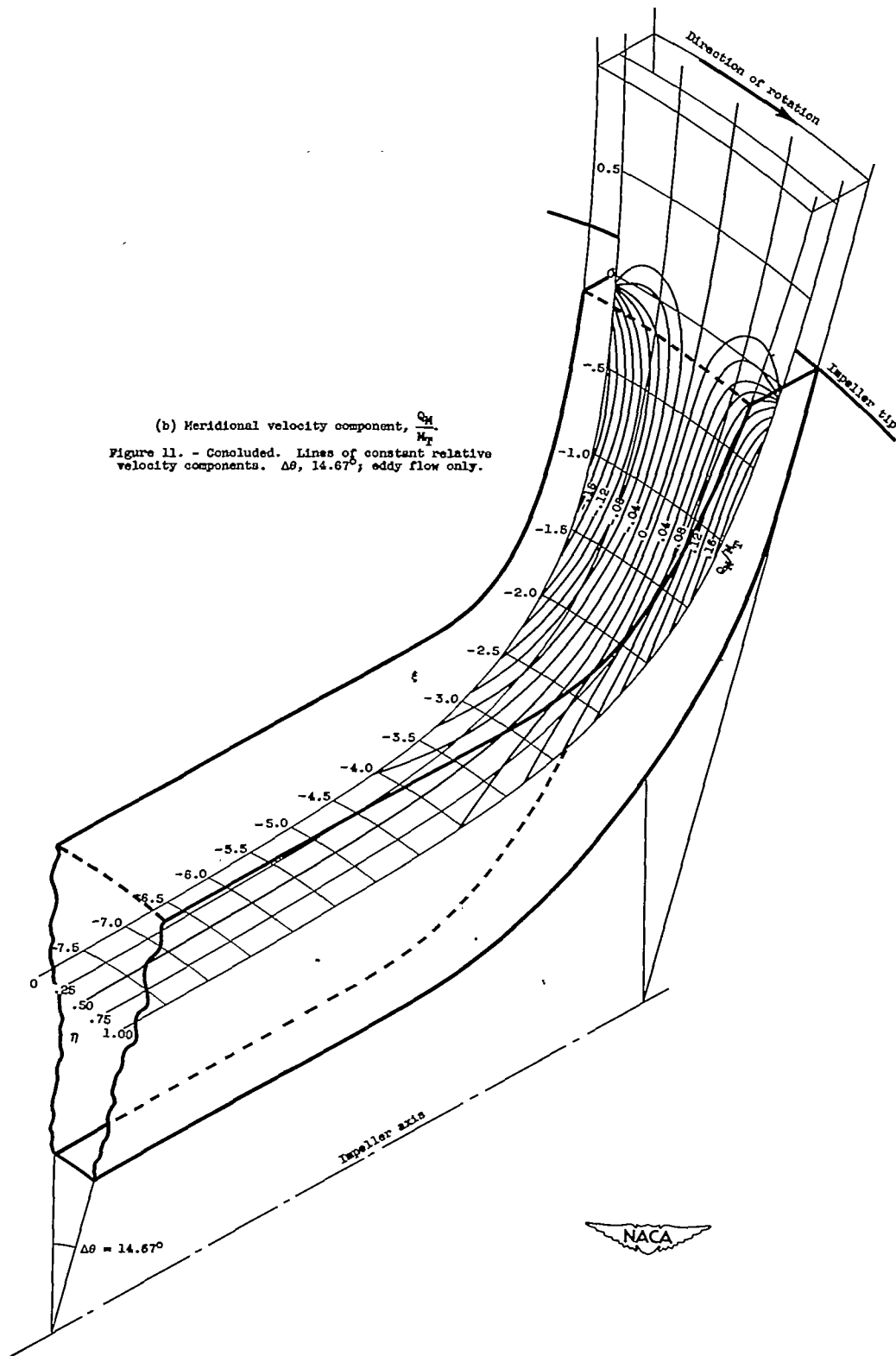


2466





2466



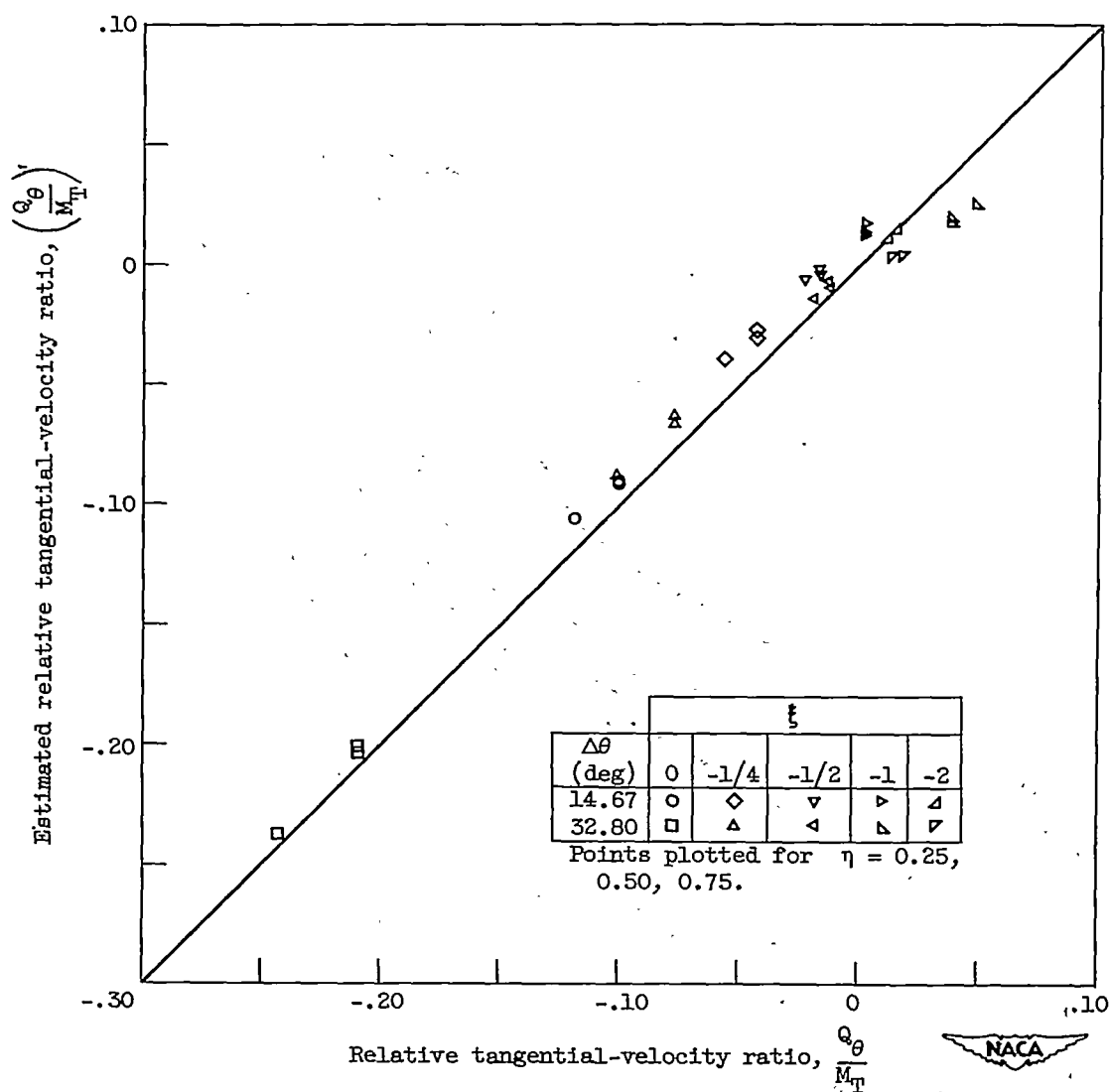


Figure 12. - Comparison between relaxation and estimated values of $\frac{Q_\theta}{M_T}$.
Correlation equation (21a).

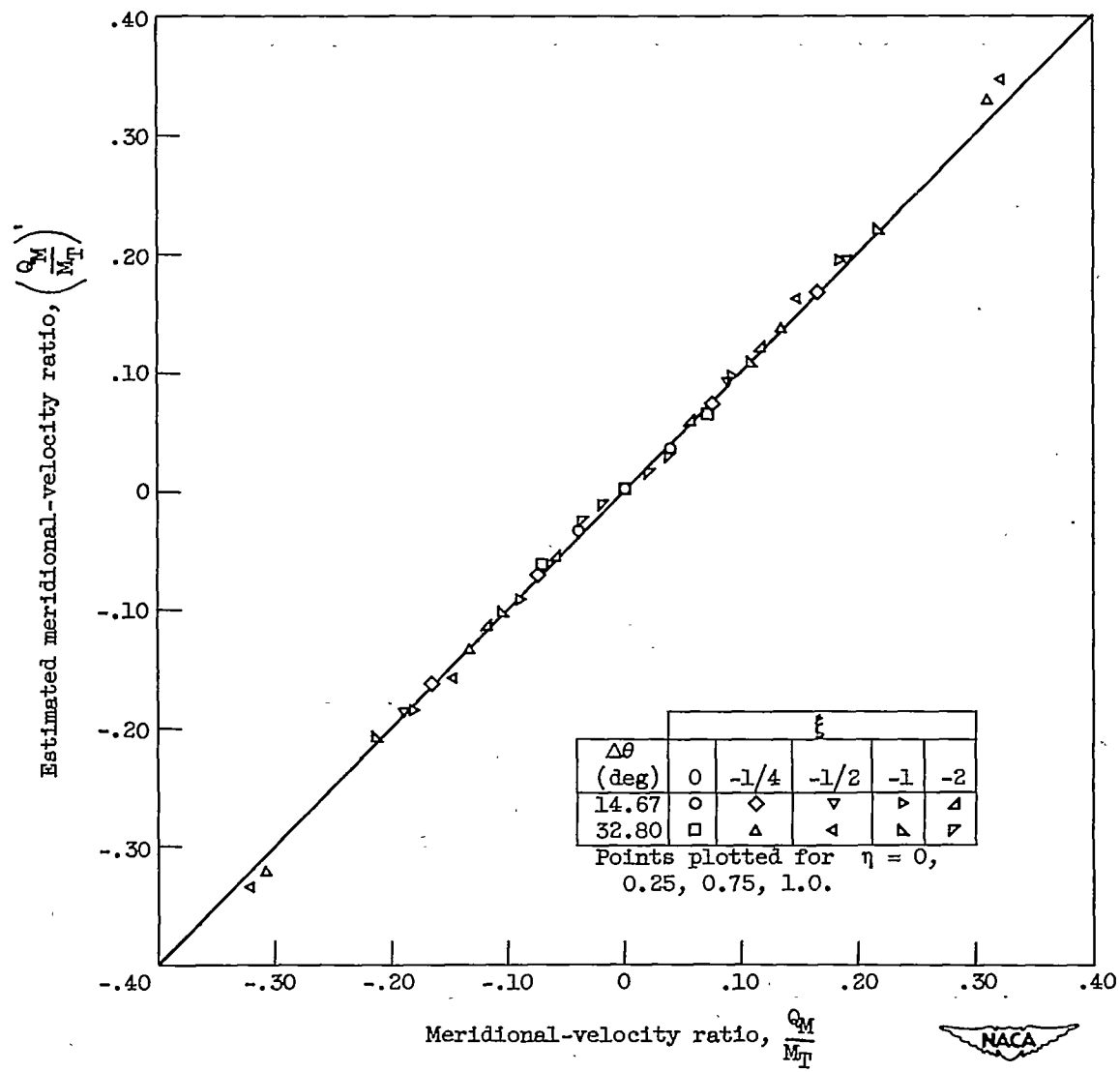


Figure 13. - Comparison between relaxation and estimated values of $\frac{Q_M}{M_T}$.
Correlation equation (23a).

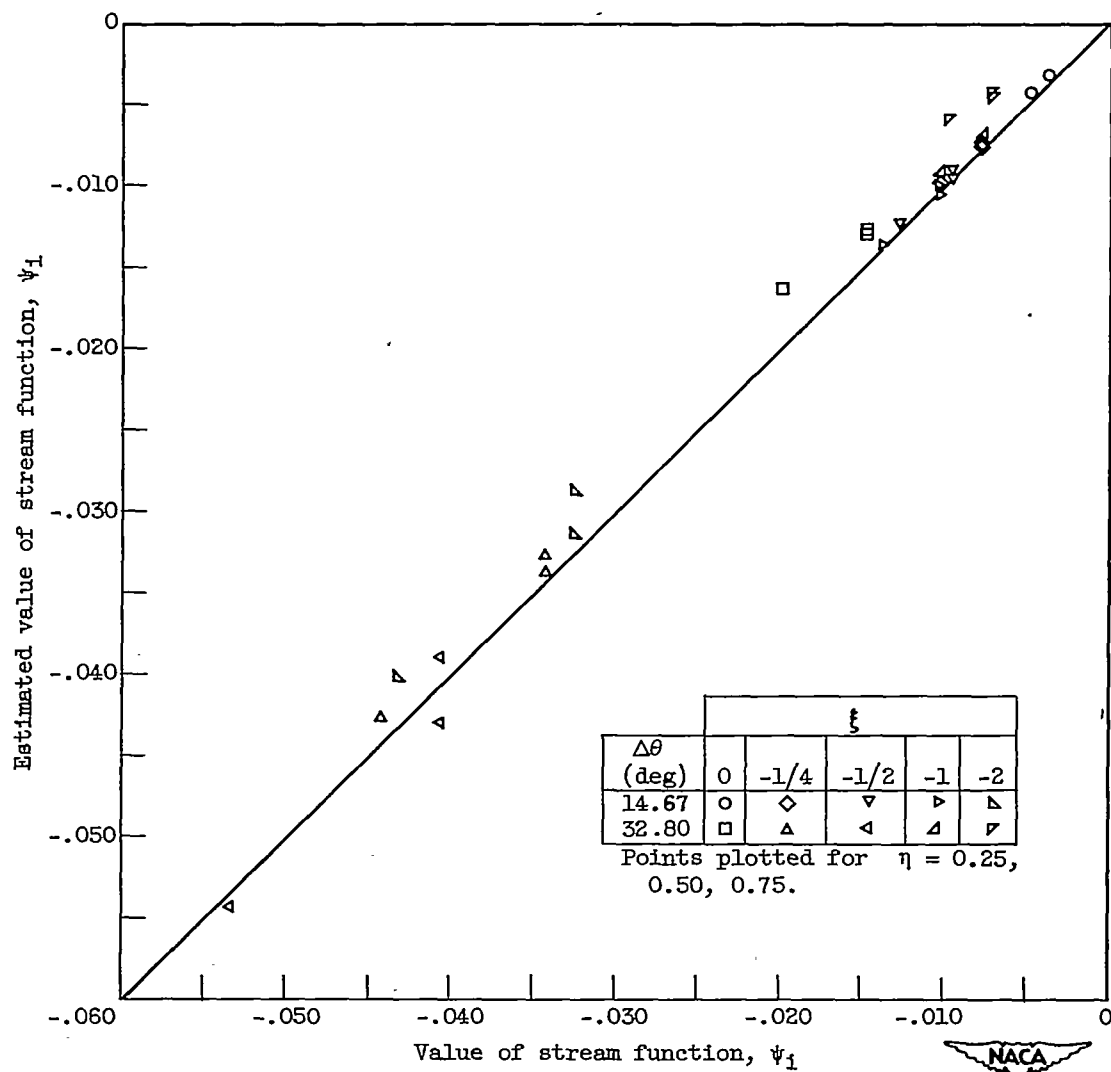


Figure 14. - Comparison between relaxation and estimated values of ψ_1 .
Correlation equation (25a).

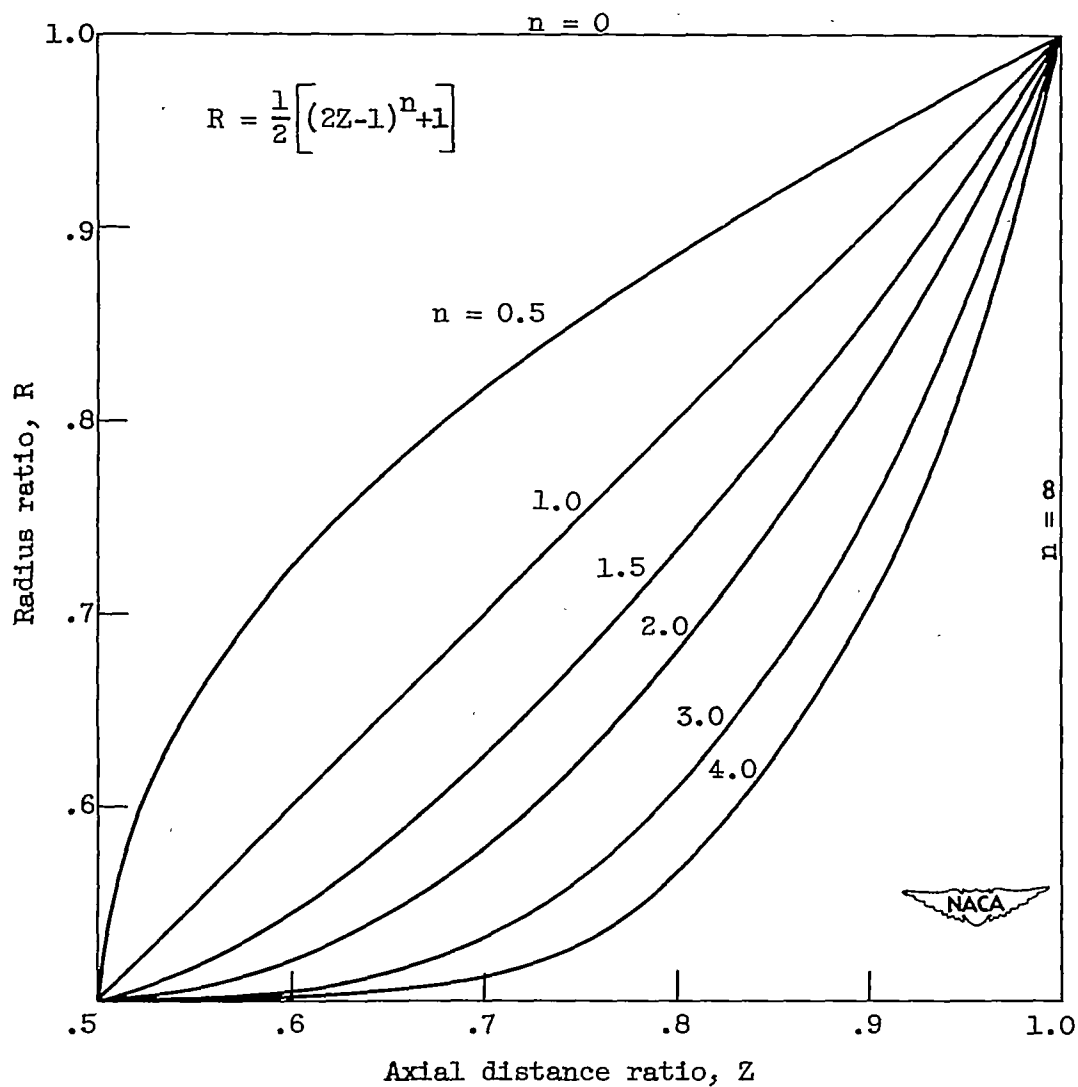


Figure 15. - Generating lines in axial-radial plane that are rotated about axis of impeller to obtain flow surfaces of revolution.

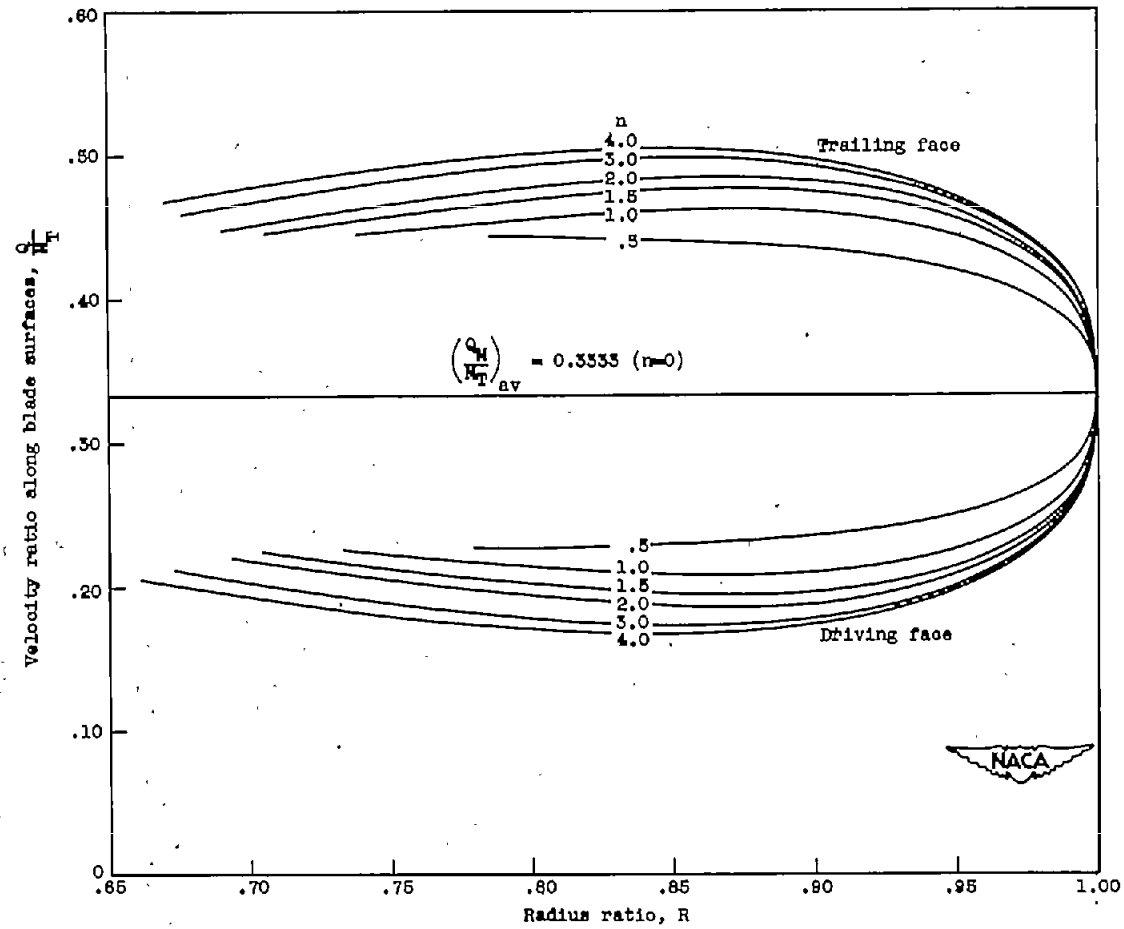


Figure 16. - Velocity-ratio along blades for various shapes of flow surface of revolution.